



Biometry and taxonomy of Adriatic *Ammonia* species from Bellaria–Igea Marina (Italy)

Joachim Schönfeld¹, Valentina Beccari², Sarina Schmidt¹, and Silvia Spezzaferrì²

¹GEOMAR Helmholtz-Zentrum für Ozeanforschung Kiel, Wischhofstrasse 1–3, 24148 Kiel, Germany

²Department of Geosciences, University of Fribourg, Chemin du Musée 6, 1700 Fribourg, Switzerland

Correspondence: Joachim Schönfeld (jschoenfeld@geomar.de)

Received: 22 July 2021 – Revised: 18 October 2021 – Accepted: 19 October 2021 – Published: 25 November 2021

Abstract. Living *Ammonia* species and an inventory of dead assemblages from Adriatic subtidal, nearshore environments were investigated at four stations off Bellaria, Italy. *Ammonia falsobeccarii*, *Ammonia parkinsoniana*, *Ammonia tepida*, and *Ammonia veneta* were recognized in the living (rose-bengal-stained) fauna, and *Ammonia bellaria* n. sp. is described herein for the first time. *Ammonia beccarii* was only found in the dead assemblage. The biometry of 368 living individuals was analysed by using light microscopic and scanning electron microscopic images of three aspects. A total of 15 numerical and 8 qualitative parameters were measured and assessed, 5 of which were recognized to be prone to a certain subjectivity of the observer. The accuracy of numerical data as revealed by the mean residuals of parallel measurements by different observers ranged from 0.5 % to 5.5 %. The results indicated a high degree of intraspecific variability. The test sizes of the individual species were log-normally distributed and varied among the stations. Parameters not related to the growth of the individuals, i.e. flatness of the tests, dimensions of the second-youngest chamber, proloculus, umbilical and pore diameter, sinistral–dextral coiling, and umbilical boss size, were recognized as being species-distinctive in combination. They may well supplement qualitative criteria that were commonly used for species discrimination such as a lobate outline, a subacute or rounded peripheral margin, or the degree of ornamentation on the spiral and umbilical sides. The averages of the measured parameters were often lower than the range of previously published values, mainly because the latter were retrieved from a few adult specimens and not from the whole assemblage as in the present approach. We conclude that the unprecedented high proportions of *Ammonia beccarii* in the northern Adriatic may well be artificial. A robust species identification without genetic analyses is possible by considering designated biometric parameters. This approach is also applicable to earlier literature data, and their re-assessment is critical for a correct denomination of recent genotypes.

1 Introduction

Species of the genus *Ammonia* Brünnich (1772) are deemed important members of benthic foraminiferal assemblages in intertidal to outer shelf environments worldwide (Murray, 1991). They show significant proportions in both living faunas and dead assemblages (e.g. Donnici and Barbero, 2002; Diz and Francés, 2008; Francescangeli et al., 2021). The species occupy a variety of microhabitats and may facultatively exploit different food sources; some are mobile and quite fast (Richter, 1961; Langer et al., 1989; Debenay et al., 1998; Pascal et al., 2008; Dupuy et al., 2010; Seuront and

Bouchet, 2015; Haynert et al., 2020). Some *Ammonia* species show a high tolerance to salinity and temperature variations in laboratory experiments and natural environments (Bradshaw, 1961, 1968; Stouff et al., 1999a). They may stand only moderate levels of organic carbon enrichment, avoid hypoxia, or fall into dormancy under anoxic conditions (de Chanvalon et al., 2015; LeKieffre et al., 2017; Bouchet et al., 2021).

Shallow-water environments have been the particular focus of foraminiferal studies of the last decades (e.g. Murray, 2015). Taxonomical, distributional, and ecological investigations prevailed but only a few *Ammonia* species names were

used, e.g. *Ammonia batava*, *A. beccarii*, *A. parkinsoniana*, or *A. tepida*, despite differences in climatic or hydrodynamic conditions or different bioprovinces (e.g. Walton and Sloan, 1990; Hayward et al., 2004). Genetic investigations revealed a high level of cryptic diversity, in particular in the plexus of the morphospecies *A. tepida* (e.g. Holzmann, 2000). Genotypes or operational taxonomic units (OTUs) denominated open nomenclature (Holzmann and Pawlowski, 1997). This is commonly pursued in life sciences but indicates the possibility that the same acronym is introduced for two different species (e.g. sp. T1; Deldicq et al., 2019).

In a first comprehensive compilation, Hayward et al. (2004) attempted to clarify the taxonomic status of several OTUs affiliated with the genus *Ammonia*. Their recommendations were applied, challenged, rejected, and continuously applied (e.g. *A. aomoriensis*; Schweizer et al., 2011; Sen and Bhadury, 2016; Bird et al., 2020; Li et al., 2020). This created much confusion and promoted the preferential use of genotype denominations, even without supporting genetic analyses (e.g. de Nooijer, 2007; Keul et al., 2013; Koho et al., 2018). Recently, Hayward et al. (2019, 2021) re-described and denominated 67 *Ammonia* species and genotypes, partly using different names as in their first compilation. Ranges of morphometric characteristics useful for species determination were provided (Hayward et al., 2004). Other biometric approaches assessed the same characteristics and demonstrated that only the pore diameter and the suture elevation in the central part of the spiral side may facilitate a secure species differentiation, in particular among three morphologically similar genotypes (Richirt et al., 2019, 2021).

Environmental applications and biomonitoring studies using foraminifera are on the rise (e.g. Bouchet et al., 2012; Barras et al., 2014; Alve et al., 2019; Parent et al., 2021). The FORaminiferal BIO-MONitoring (FOBIMO) working group has demonstrated that a unified use of species names is essential for reliable ecosystem quality assessments (Alve et al., 2016; Jorissen et al., 2018; Bouchet et al., 2021). Consequently, recent taxonomic studies of *Ammonia* and other ecologically important genera combined a molecular characterization with morphological analyses to counter incorrect species assignments and flawed ecological interpretations (e.g. Darling et al., 2016; Bird et al., 2020). Particular emphasis was given to topotypic specimens (Roberts et al., 2016). An accurate reference to morphologically defined species concepts and type material is essential for both recent field studies and applications to the fossil record.

Ammonia beccarii Linné (1758) is the oldest and probably one of the most frequently used species names of this genus (Hayward et al., 2019). The type specimens for the drawings of “*Cornu Hammonis*” by Janus Plancus (1739) were lost. The beach off Rimini was later constrained as a type locality of the species (Cushman, 1928; Cifelli, 1962). A re-sampling of the site at wading depth in 2006 and 2018 did not retrieve any living specimens of *A. beccarii* (Hayward et al., 2019, and Bruce W. Hayward, personal communica-

tion, 2018). However, living (rose-bengal-stained) specimens were reported from two nearshore surface samples from water depths of 13 and 21 m as well as 15 and 19 km to the north of Rimini (Haake, 1977), and the species is frequent in Venice lagoon and offshore of the Po River delta between depths of 5 and 13 m as well (Donnici and Barbero, 2002; Barbero et al., 2008). Furthermore, Rimini Beach has been augmented and re-shaped at least three times since 2002. The sand used for beach nourishment has been dredged from late Pleistocene relict beaches located ca. 55 km offshore at a water depth of 40–42 m (extraction site C1; Preti 2000; Simonini et al., 2005; Montanari and Marasmi, 2012; Prioli, 2021). With reference to the recent distribution of *A. beccarii* in the Adriatic, it is conceivable that the sand accumulation site was not a suitable habitat for this species 8000 to 11 000 years ago, and neither is the touristic, managed beach today.

The motivation of the present study was to fill the gap of knowledge between littoral and nearshore environments, with particular focus on the shallowest occurrences of living *A. beccarii* close to the type locality. In a comprehensive approach, the biometry of all specimens from the living fauna was assessed, provided they were sufficiently well preserved, to gain more insight into the ontogenetic expression of distinctive morphological characteristics. We also explored which biometric features were arbitrary across the species and which were distinct and suitable for species characterization.

2 Material and methods

2.1 Sampling

Samples were collected on 5 January 2019 in coastal shallow waters of less than 3 m depth off Bellaria–Igea Marina (Rimini, Emilia Romagna, Italy). Four locations were chosen in representative parts of the area: in the channel between two lines of breakwaters (Station 1), directly in front of the breakwaters (Station 2), outside the breakwaters (Station 3), and close to the low water line (Station 4) (Fig. 1, Table B1).

Surface sediments samples were collected by using an Ekman–Birge box corer (15 × 15 × 30 cm), which was deployed from a small lifeguard boat operated by two persons. The foraminiferal samples were collected and treated following the FOBIMO protocol (Schönfeld et al., 2012). The samples were considered external replicates because they were taken at a short distance from the same environment (Hayek et al., 2021). The first centimetre of the sediment in the box core was scooped in an area of 50 cm², collected in plastic bottles, preserved, and stained with an ethanol–rose bengal solution (2 g L⁻¹, alcohol concentration 80 %). Temperature and salinity of the near-surface water were measured immediately after the collection of the last sediment sample at Station 4 by using a handheld multiparameter meter

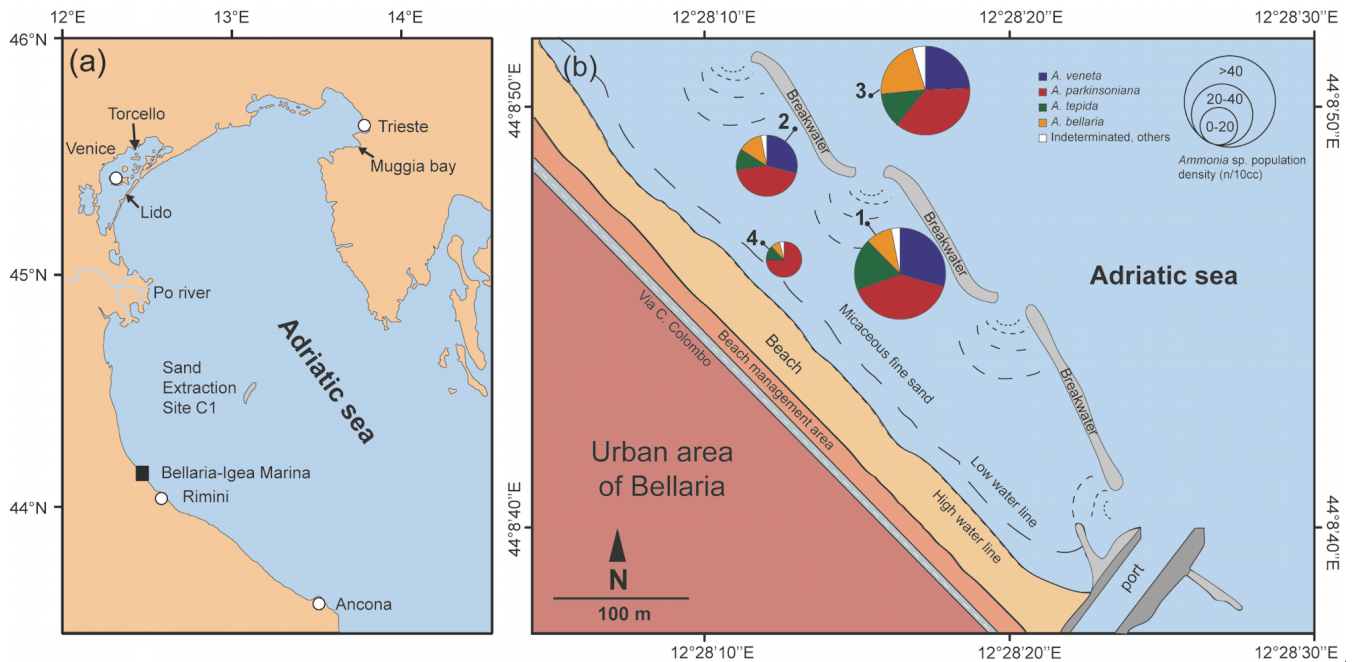


Figure 1. (a) Overview map of the northern Adriatic Sea with locations mentioned in this paper; (b) detailed map and proportions of *Ammonia* species off Bellaria–Igea Marina. The local map was drawn after satellite images and own observations. The dashed lines delineate backwash scours at the gaps between breakwaters.

Orion™ Star A325 equipped with an Orion™ DuraProbe™ 013010MD sensor for conductivity.

2.2 Sample preparation and image acquisition

The sample preparation and analyses were performed at the Department of Geosciences, University of Fribourg, Switzerland, 3 weeks after collection to ensure that the cytoplasm of foraminifera that were living at the time of the collection was sufficiently stained with rose bengal. The volume of each sediment sample was noted, and the samples were gently washed with tap water through a 32 µm mesh sieve. Thereafter, the residue from each sample was homogenized in a wet stage. An aliquot of 20 cm³ was filled in a graduated vessel with a spoon and air-dried. The aliquots were dry-picked completely for well-stained *Ammonia* specimens under a Nikon SMZ18 binocular microscope at 40 × magnification. A total of 12 exceptionally large specimens from the dead assemblage of Station 1 and a few other common benthic foraminifera were also picked for imaging. All individuals from a particular station were collected in separate Plummer cell slides, in which the *Ammonia* specimens were separated and each received a single specimen identifier.

The *Ammonia* specimens were oriented with the spiral side up using a wet paintbrush. They were photographed for a first screening and biometric measurements with a Nikon SMZ18 stereo microscope equipped with a digital camera in a wet stage to enhance the staining pattern. Subsequently, the imaged specimens were mounted on nine different scanning

electron microscope (SEM) stubs. Between 30 and 60 specimens were arranged on each stub, depending on the test sizes. The stubs were coated with 40 nm of gold. Scanning electron microscope images were taken with a Thermo Fisher SEM FEI XL30SFEG upgraded to remX Microscope Control at 20 keV voltage. The spiral side of all specimens was imaged first. Then the specimens were turned on the umbilical side, detaching them gently from the glue and the gold coating with a wet paintbrush, and repositioning them in the same order on a new SEM stub. The specimens were coated again and imaged, and then the process was identically repeated for the apertural side.

2.3 Image analyses and species identification

2.3.1 Light microscope images

Light microscopic images of the spiral side had a size of 2836 × 2037 pixels, 32 bit colour depth, and 17.5 to 17.8 MB in tagged image file format (TIFF). They were first customized to an average size of ca. 800 × 100 pixel (ca. 2.9 MB), and the specimens were rotated with the latest chamber upwards. The operations and measurements were performed with GraphicConverter© version 7x (Lemke Software, Peine, Germany) on Apple Macintosh® computers. The resolution ranged from 2.8 to 6.3 pixel µm⁻¹. The biometrical measurements on the images were carried out following Hayward et al. (2004, their Plate 1) and Richirt et al. (2019, their Fig. 3) (Table B2). The greatest test diam-

eter, average diameter of the proloculus, length and height of the second chamber, proportion of smooth outline of the test, the angle between the spiral suture and the suture of the second and third chamber, the total number of chambers, the number of chambers of the last whorl, and the coiling direction were measured or assessed. An assessment of the degree of inflation of the final chambers shaping the periphery outline was found to be highly subjective. Therefore, we only discerned between a smooth and lobulate outline. The pore size could only be estimated as rather large or small. Microspheric and macrospheric individuals were identified. Once the final chamber was broken off or certain features could not be made visible by tuning the brightness and contrast of the image, the test diameter or respective parameter was not recorded. The images were analysed by up to three different observers, and mean values were used for further analyses. The individual accuracy is of the order of $\pm 3\%$ (two observers, mean residual of 15 parallel measurements of the proloculus diameter in specimen nos. 123–140).

2.3.2 SEM images

SEM images had a size of 4000×3000 pixels, 8 bit colour depth greyscale, and 12.9 MB in TIFF. They were also customized prior to analyses, in particular rotated with the latest chamber upwards for spiral and umbilical side aspects and orientated horizontally for the apertural aspect. The images were analysed by one or two observers, and mean values were used for further analyses. The operations and measurements were performed with GraphicConverter© and Adobe® Illustrator©. The resolution depended on the magnification and varied between 2.8 and $6.4 \text{ pixel } \mu\text{m}^{-1}$ for the spiral side, 0.6 and $24.8 \text{ pixel } \mu\text{m}^{-1}$ for the umbilical side, and 2.7 and $23.1 \text{ pixel } \mu\text{m}^{-1}$ for the apertural side images. The greatest test diameter, length and height of the second chamber, extension of the spiral fissure, the angle between the spiral suture and the suture of the second and third chamber, the presence of raised calcite ridges on radial sutures, and the pore diameter on the second chamber were measured and assessed on images of the spiral side. For pore diameter measurements, we simplified the approach of Richirt et al. (2019) and applied a point-counting method (e.g. Chayes, 1949, and references therein). In particular, a line was drawn parallel to the spiral suture near the bottom of the second chamber, and the diameter of 13 subsequent pores on or very close to the line was measured. The mean value of these measurements was used for further analyses. On images from the umbilical side, the diameter of the umbilicus between ends of opposite folia, the number of umbilical bosses, the average diameter of the largest boss, the relative length of the third radial sutural furrow, the presence of beads along the edge of radial sutures, the presence of pustules, calcite ridges, or knobs on folia, and whether the folia were curved or straight were measured or assessed. On apertural images, the greatest diameter and the heights of the spiral and umbilical side were mea-

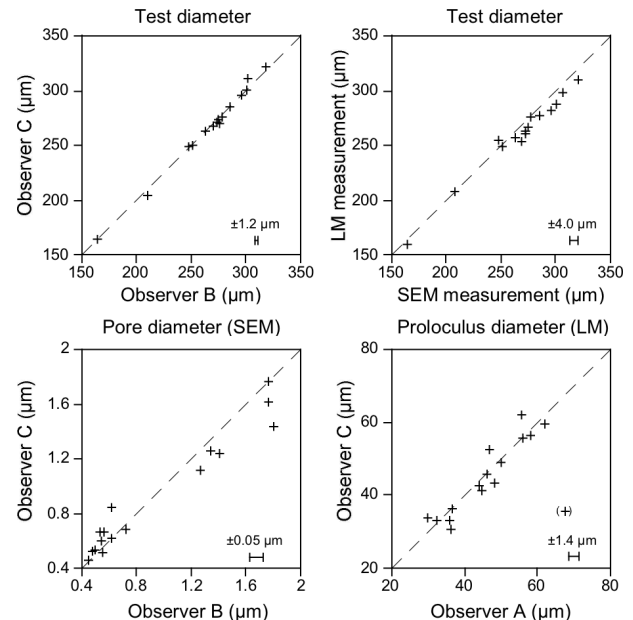


Figure 2. Parallel measurements of the greatest test diameter, mean pore diameter, and proloculus diameter of specimen nos. 123–140 by two different observers, SEM, and light microscopic (LM) measurements. The dashed line depicts the position of coincidence, and the error bars show the residual mean. The value in brackets was visually identified as an outlier and was not included in the calculations. Note the higher variability of pore diameter and light microscopic measurements.

sured, and the flatness and convexity of the spiral side were calculated.

The precision of the SEM measurements was assessed with a Sira test object showing $19.7 \text{ lines mm}^{-1}$. The mean difference between target and measured values was -0.20% and -0.22% of the target value in the horizontal and vertical direction at 200- to 800-fold magnification and is thus considered negligible. The individual accuracy of the measurements on SEM images ranged from $\pm 0.4\%$ of the greatest test diameter to $\pm 5.5\%$ of the mean pore diameter (two observers, mean residual of 15 parallel measurements in specimen nos. 123–140) (Fig. 2). With reference to the greatest test diameter, the measurements on SEM images were on average higher by 1.4% compared to measurements on the corresponding light microscopic images, depicting the lower precision of the light microscope.

The *Ammonia* specimens were not sorted by species in the Plummer cell slides before imaging to avoid damage and accidental loss of specimens during the operations. As such, the individuals could not be determined and counted by species prior to imaging. Furthermore, their species affiliation could not be discussed in person among the participants of the present study due to Covid-19 travel and contact restrictions. Therefore, copies of the SEM images were re-oriented, scaled down to a size of $2 \times 2 \text{ cm}$ at 300 dots per

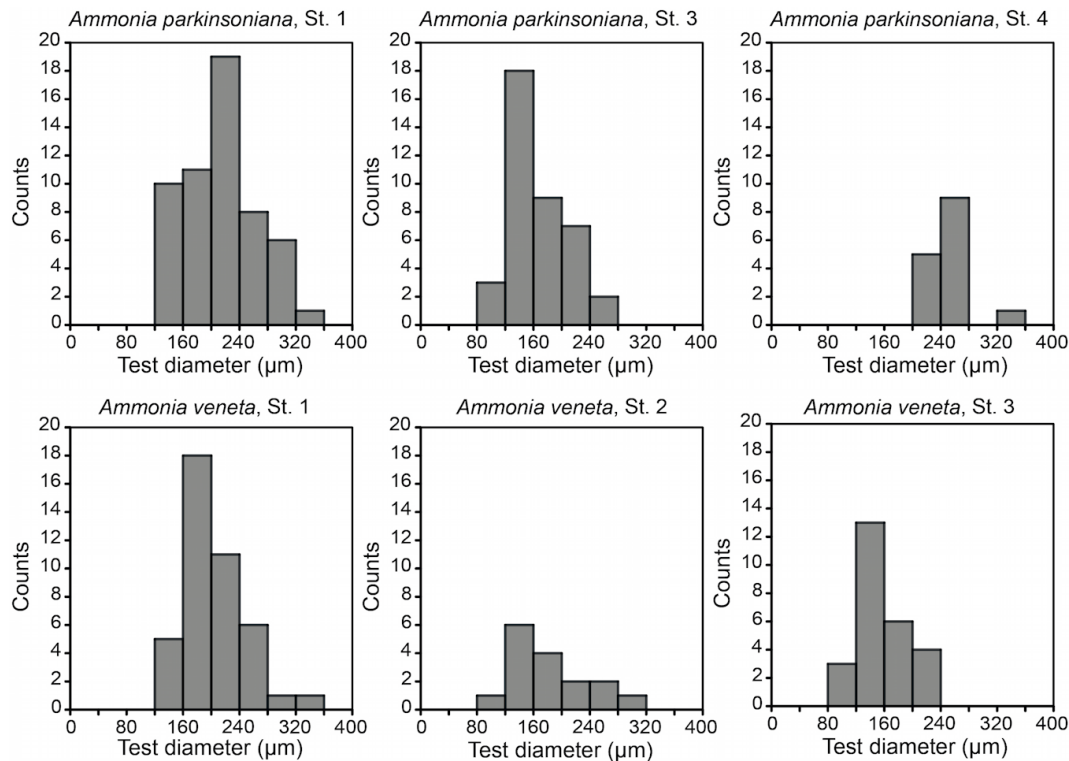


Figure 3. Size distribution of *Ammonia veneta* and *Ammonia parkinsoniana* at Stations 1 to 4. *Ammonia veneta* is absent at Station 4.

inch (dpi) resolution, and arranged in a Microsoft Word® table with the identifier, spiral side image, umbilical side, and apertural side image of each specimen. The specimens were determined by each observer, mainly by referring to SEM images of recent literature and the Ellis and Messina (1940) catalogue. The tables were re-arranged, and the determinations of those specimens were repeated when a consensus could not be achieved. This procedure was repeated several times. Finally, a large table was mounted with the specimens designated to a particular species, and the determination was approved by all authors.

2.4 Data analyses and statistics

Biometric data depending on the volume of spherical objects, such as foraminiferal chambers, are usually log-normally distributed. Therefore, the non-parametric Wilcoxon Mann–Whitney test and not the Student’s *t* test was performed to address whether the intact and the broken foraminiferal tests differ significantly from each other. Single parameters of broken and intact specimens within a species were compared. Furthermore, the Wilcoxon Mann–Whitney test was used to analyse if parameters within a species statistically differ between the different sampling stations. All statistical analyses were carried out with the programme PAST (Hammer, 2001).

Log-probability plots were used to identify potential subpopulations within a species, which would influence the interpretation of the morphological characteristics measured in this study. Normal or log-normal distributions are depicted by a straight line (Otto, 1939), and a change in their slope indicated by a break can be used for separating the subpopulations (Schönfeld and Voigt, 2020).

3 Results

3.1 *Ammonia* assemblage composition and distribution

Five different *Ammonia* species were recorded in the living (rose-bengal-stained) fauna of the four sampling stations ranging from water depths of 0.5 to 3 m (Tables B1, B3). *Ammonia beccarii* was only found in the dead assemblage of Station 1 at a depth of 2 m. In total, 393 living specimens were imaged, 379 of which could be determined in consensus.

Ammonia parkinsoniana was identified by its less lobate and rounded peripheral outline, the large umbilical knob, smooth sutures on the spiral side, and small, indistinct pores. *Ammonia veneta* showed thickened and raised sutures on the spiral side, markedly coarse pores, and pustules on the umbilical extensions of earlier chambers on the umbilical side. *Ammonia tepida* was identified by the marked lobate outline and rounded peripheral margin, smooth sutures and

less numerous chambers on the spiral side, umbilical folia with protoforamina, and the angular space between sutures in the umbilical area. The pores were small. *Ammonia bellaria* n. sp. showed a biconvex profile with a subacute peripheral margin, a rosette-like chamber arrangement on the spiral side, a very small knob, and only few pustules on the narrow umbilical area. *Ammonia falsobeccarii* was identified by its supplementary apertures on the spiral side. *Ammonia beccarii* was markedly different to all other *Ammonia* species (Appendix A). It showed more numerous chambers in the last whorl and transverse pustules and ridges on the spiral side, a well-developed keel, a knob, and strong ornamentation around the umbilicus including beads along the edges of radial sutures (Table B6e).

The standing stock of *Ammonia* species varied between 12 and 82 individuals per 10 cm³. The highest values were recorded at Stations 1 and 3, in the channel deep between breakwaters, and outside the breakwaters (Fig. 1). *Ammonia parkinsoniana*, *A. veneta*, and *A. tepida* were the first, second, and third ranked species. They showed rather constant proportions, whereas *A. bellaria* n. sp. was comparatively variable. At Station 4 close to the low water line, *A. veneta* was missing and the standing stock was very low. One living specimen of *Ammonia falsobeccarii* was recorded at this station only.

The salinities and temperatures were 36.09 units and 7.3 °C at Station 4, which is in agreement with nearshore settings in the northern Adriatic Sea during winter. The surface water temperatures may rise up to 23 °C in summer, while the salinities show a strong spatial variability. They are mainly controlled by frontal processes and freshwater influx from the Po River and other rivers (e.g. Artegiani et al., 1997). Nonetheless, winter is the time of highest environmental stability, after the touristic season and before storms and enhanced freshwater influx during spring. The tidal range in the area was ±0.60 m. The nearshore surface sediment was a micaceous fine sand. Wave-originated ripple marks were common, and filamentous green algae and *Ulva* were abundant in places.

3.2 Biometric data quality assessment

From the living *Ammonia* assemblages, 368 specimens were measured. The measurements of 11 specimens were discarded because the spiral side and apertural aspect showed a markedly different diameter or they were erroneously assigned to *Haynesina* species. The individuals were mostly well preserved. Features of corrosion or abrasion and repair structures were recognized on a few specimens only. Nonetheless, sample preparation or specimen manipulation caused damage of 55 % of all individuals. The most frequent damage was the loss of the final chamber. Others were spoilt with glue during re-orientation on the SEM stubs, or they were lost during transfer or gold coating. Therefore, not all parameters could be assessed on these individuals. The

Wilcoxon Mann–Whitney tests revealed no significant differences between the data distribution of the respective parameters in the 201 damaged and 167 well-preserved specimens. Exceptions are the umbilicus, umbilical boss, and proloculus diameter in *A. parkinsoniana* (Table B4), which may depend on the test size of the specimen. Considering these exceptions, it is justified to augment the biometric data on intact specimens by values of broken individuals. The biometric data on intact specimens are likewise considered to be representative for the entire assemblage of well-preserved and damaged specimens.

A total of 22 different parameters were measured and assessed, 5 of which are distance measurements, 1 an angle, 3 ordinates, 6 ratios, and 7 qualitative parameters (Table B2). Parallel measurements revealed that ratios and qualitative parameters were prone to a certain degree of subjectivity among the observers, e.g. where the radial or spiral fissure exactly ends, whether ridges or knobs on folia were weak or strong, and whether the folia were straight or rather slightly curved. For instance, two observers achieved a consensus of 81 % on the latter parameter and individual nos. 123–140. Other qualitative parameters were proven reliable, e.g. left or right coiling. We therefore decided to use only data for species discrimination for which the variability is rather governed by the measurement accuracy than by personal judgement or preservation.

The maximum test diameter is particularly important to investigate the state of a foraminiferal population. The size distribution of a certain species is moulded by different cohorts generated during distinct reproduction events or by instantaneous reproduction (Murray and Alve, 2000). The expression of diagnostic morphological characteristics is often a matter of ontogenetic stage (e.g. Raw, 1925; Bé, 1959). It is therefore important to assess whether the size distribution among the samples is significantly different or not before the entire data set is analysed.

The test diameters of the first ranked species *A. veneta* and *A. parkinsoniana* showed a left-skewed size distribution with maxima in different size classes. The histograms did not reveal different cohorts generated by certain reproduction events (Fig. 3). Plotted on a log-probability scale, the test diameters of *A. veneta* and *A. parkinsoniana* showed a log-normal distribution in all samples (Fig. 4). The log-probability curves displayed numerous inflexions comprising 2 to 5 data points, which indicate small subpopulations of a few specimens. The size distribution curves of *A. veneta* at Stations 1 and 2 were very similar at a test diameter >200 µm, whereas they diverged at smaller diameters. This is also mirrored by the low *p* value of the Wilcoxon Mann–Whitney test (Table B4). The populations of *A. parkinsoniana* were almost identical at Stations 1 and 2. The shape of the curves of both species from Station 3 was almost identical, although it was offset to smaller sizes by a few tens of microns. The size distribution curve of *A. parkinsoniana* from Station 4 is largely different to the distribution curves

from all other stations, which is also expressed in low p values of the Wilcoxon Mann–Whitney tests (Table B4). The distribution indicated a blend of three subpopulations with two to nine specimens of *A. parkinsoniana* at Station 4, each with a very narrow size range. For this reason and the fact that *A. veneta* is absent at this station closest to the shore, we excluded the biometric data from Station 4 and merged the biometric data from Stations 1 to 3 by species for all subsequent analyses.

3.3 Ontogenetic development of characteristics

Numerical biometric parameters were investigated for a relationship with the maximum test diameter in order to identify possible ontogenetic influences on the expression of these characteristics (Fig. 5). Only biometric data from intact specimens were considered to ensure comparability of confidence levels among the parameters. The intact specimens were proven to be representative for the whole population as demonstrated above. The data showed considerable scatter, and therefore a significance level of 99 % was chosen ($p \leq 0.01$).

The number of chambers and the umbilicus diameter showed a significant positive correlation with the test diameter in *A. veneta*, *A. parkinsoniana*, and *A. tepida*. Convexity of the test, dimension of the second chamber, extension of the spiral fissure, and mean pore diameter showed a significant positive relationship with the test diameter of *A. veneta* as well (Table B5). Flatness, umbilical boss, and proloculus diameter significantly correlate with the test diameter of *A. parkinsoniana*. A correlation with the proloculus diameter is also established in *A. tepida*. *Ammonia bellaria* n. sp. only showed a significant correlation of the dimension of the second chamber with the maximum test diameter in that the chambers are substantially longer in large adult specimens (Table B5).

All these relationships appeared to be linear with the exception of the umbilicus diameter in *A. tepida*. Presumably juvenile specimens with a diameter $< 200 \mu\text{m}$ showed umbilical diameters $< 28 \mu\text{m}$, whereas specimens with a diameter $> 250 \mu\text{m}$ had a substantially larger umbilical diameter $> 54 \mu\text{m}$ (Fig. 5). Interestingly, and with one exception, the proportion of a smooth outline was much lower in the small (0 %–43 %) than in the large individuals (62 %–90 %). The juveniles thus showed a lobate periphery, whereas the adults showed a smooth outline and only the final chambers were inflated.

3.4 Species discrimination

The ranges of maximum test diameters showed a large overlap of *A. veneta*, *A. parkinsoniana*, and *A. tepida*, and their mean values were also very similar with $173 \mu\text{m}$ ($\pm 72 \mu\text{m}$, 1σ) to $199 \mu\text{m}$ ($\pm 52 \mu\text{m}$, 1σ) (Table B6). *Ammonia bellaria*

n. sp., however, was markedly smaller with a mean diameter of $131 \mu\text{m}$ ($\pm 22 \mu\text{m}$, 1σ).

The ratio of diameter and height of the test indicates whether the test is rather flat or stout. The data distribution patterns of *A. veneta*, *A. tepida*, and *A. bellaria* n. sp. were very similar (Fig. 6). Only *A. parkinsoniana* showed distinctively flatter tests than the other species, even though they were not larger than *A. veneta* and *A. tepida*. The ratios of length and width of the second chamber showed that the chambers were on average wider than long in *A. parkinsoniana*, about in equal dimensions in *A. veneta*, and distinctively longer in *A. tepida* and *A. bellaria* n. sp.

Microspheric individuals were depicted by a very small proloculus diameter ($< 20 \mu\text{m}$) and an exceptionally high total number of chambers (Fig. 5). The figures indicated that microspheric specimens were 2 % rather rare in *A. veneta* and *A. parkinsoniana*. They with 8 % and 13 % more common in *A. tepida* and *A. bellaria* n. sp. The proloculus diameter of the megalospheres was on average slightly lower in *A. parkinsoniana* than in *A. veneta* and again lower in *A. tepida* and *A. bellaria* n. sp. (Fig. 6) (Table B6).

The umbilical diameter correlates with the test diameter in *A. veneta*, *A. parkinsoniana*, and *A. tepida*, and thus the data distribution showed a comparable pattern. The data range is far lower in *A. bellaria* n. sp. even though the mean value and median correspond to that of *A. tepida*. An umbilical boss is developed in the majority of *A. parkinsoniana* (93 %) and *A. veneta* (88 %), whereas it is far less common in *A. tepida* (37 %) and *A. bellaria* n. sp. (44 %). *Ammonia parkinsoniana* showed the largest umbilical bosses with a mean diameter of $23 \mu\text{m}$ ($\pm 8.6 \mu\text{m}$, 1σ), followed by *A. veneta* and *A. tepida* with a mean diameter of $11 \mu\text{m}$ (± 4.5 and $5.4 \mu\text{m}$, 1σ). The umbilical bosses in *A. bellaria* n. sp. were slightly smaller with $8 \mu\text{m}$ on average ($\pm 2.7 \mu\text{m}$, 1σ). The mean pore diameter is much higher in *A. veneta* ($1.33 \pm 0.22 \mu\text{m}$; 1σ) than in the other species (0.51 – $0.54 \mu\text{m}$) (Fig. 6).

The ratio of sinistral and dextral tests is quite variable among the species. *Ammonia parkinsoniana* showed with 77 % the highest proportion of left-coiling specimens, followed by *A. tepida* and *A. veneta* with 57 % and by *A. bellaria* n. sp. with 43 %.

4 Discussion

4.1 Ontogenetic influences on biometric parameters

The ontogenetic stage of a specimen is parameterized by the maximum test diameter rather than by the number of chambers that have been built in the present study. The latter does not include the size of the chambers, which increases during growth, and it is biased by the difference between microspheric and macrospheric individuals. The total number of chambers is highly variable among individuals of the same diameter. For instance, adult specimens of *A. parkinsoniana* in the size range of 252 – $274 \mu\text{m}$ showed 12–18 cham-

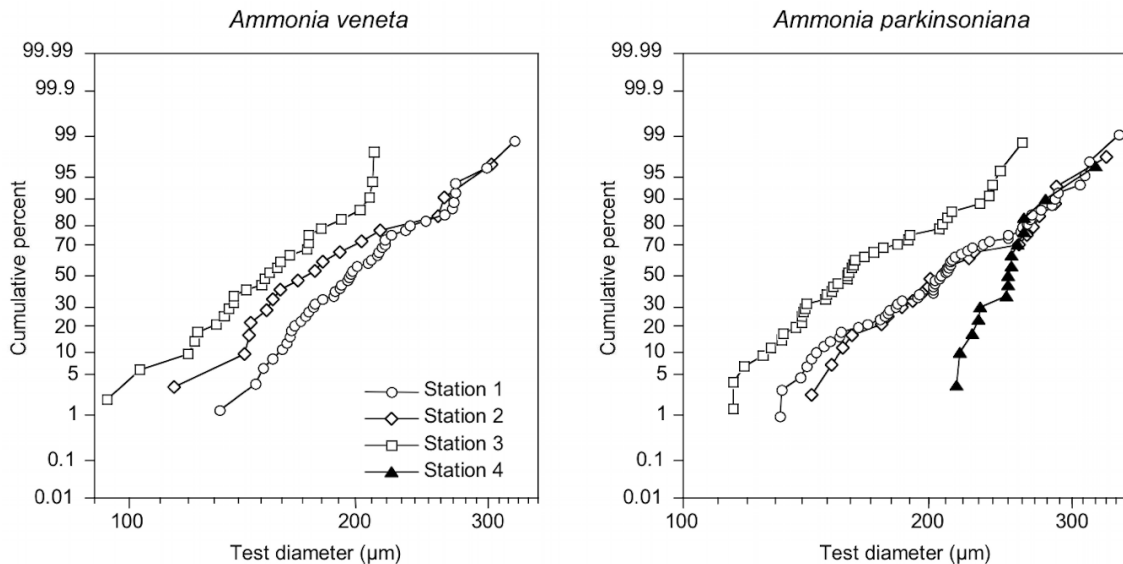


Figure 4. Size distribution of *Ammonia veneta* and *Ammonia parkinsoniana* at Stations 1 to 4 on a log-probability scale. Note the log-ordinate scale of the test diameter.

bers. This variability is not due to test abnormalities, in particular reduced or overdeveloped chambers (Myers, 1943; Polovodova and Schönfeld, 2008). In fact, only 6 of 368 (1.6%) measured specimens showed test abnormalities in the present study, which is in the range of values recorded in natural, unstressed environments (1%–3%; Alve, 1991; Polovodova and Schönfeld, 2008).

Other biometric parameters showed a high variability as well. A covariance with test size was almost not recognizable (Fig. 5), even though the correlation coefficient suggests a statistically significant relationship. Despite the number of chambers, the convexity, shape of the second chamber, and umbilicus and proloculus diameter correlate with the maximum test diameter in more than one species (Table B5). The latter parameter, however, is not a matter of ontogeny but pre-determined by the size of the megalospheric juvenile produced during asexual reproduction (gamont; Lister 1895; Lehmann, 2000; Murray, 2012). The average diameter of the proloculus may be species-specific as detailed above. The values from the present study, however, are substantially lower than those reported by Stouff et al. (1999b) from laboratory cultures of *Ammonia tepida* (50–110 µm). Nonetheless, the proloculus diameter covaried with test size. This indicates that larger gamonts grow up to larger specimens; they hence grow faster and are more competitive in food acquisition. A similar dynamic is known from fish populations (Ward et al., 2006). It is also possible that propagules have grown after reactivation from dormancy and before calcifying their initial chamber.

An ontogenetic change in test morphology is common in many foraminiferal genera and species. For instance, a change from spiral to rectilinear tests is recognized in *Am-*

motium, *Ammoscalaria*, *Ammobaculites*, and *Marginulina* species. *Dorothia*, *Muroloplecta*, and *Gaudryina* species change from triserial to biserial tests. These changes were explained by the theoretical morphospace model (Tyszka, 2006). Uniserial, biserial, or coiled morphologies are characterized by defined ranges of translation factor or length, deflection, and rotation angle of the growth vector between the earlier aperture and the middle of the newly formed chamber in a moving reference model (Labaj et al., 2003). These ranges define a morphospace of various complexity (Tyszka, 2005). A small change in one parameter exceeding a certain threshold named morphophase transition will lead to a drastic change in morphology, e.g. from biserial to uniserial or from slender to stout test shape (Tyszka et al., 2005).

For trochospiral tests like those of *Ammonia* species, however, the morphospace is extended compared to other morphophases, and thus profound changes are less likely (Tyszka, 2006). Furthermore, trochospiral taxa have minimized the distance between the aperture and the foramen of the penultimate chamber (Tyszka et al., 2005; Polovodova and Schönfeld, 2008). Therefore, the transfer of environmental stimuli from the pseudopodia to the nucleus of the cell is optimized (Hottinger, 1978; Hohenegger, 1999). This holds true for two *Ammonia* species in the present study. The convexity increases with test size in *A. veneta* keeping both the length and deflection of the growth vector constant. *Ammonia parkinsoniana* keeps the proportion of the chambers but widens the umbilicus with growth. Thereby, the flatness of the test increases and the decisive growth vector is kept constant by successively reducing the rotation angle. Both strategies ensure a fast responsiveness of large individuals to environmental signals, which is essential in systems of high

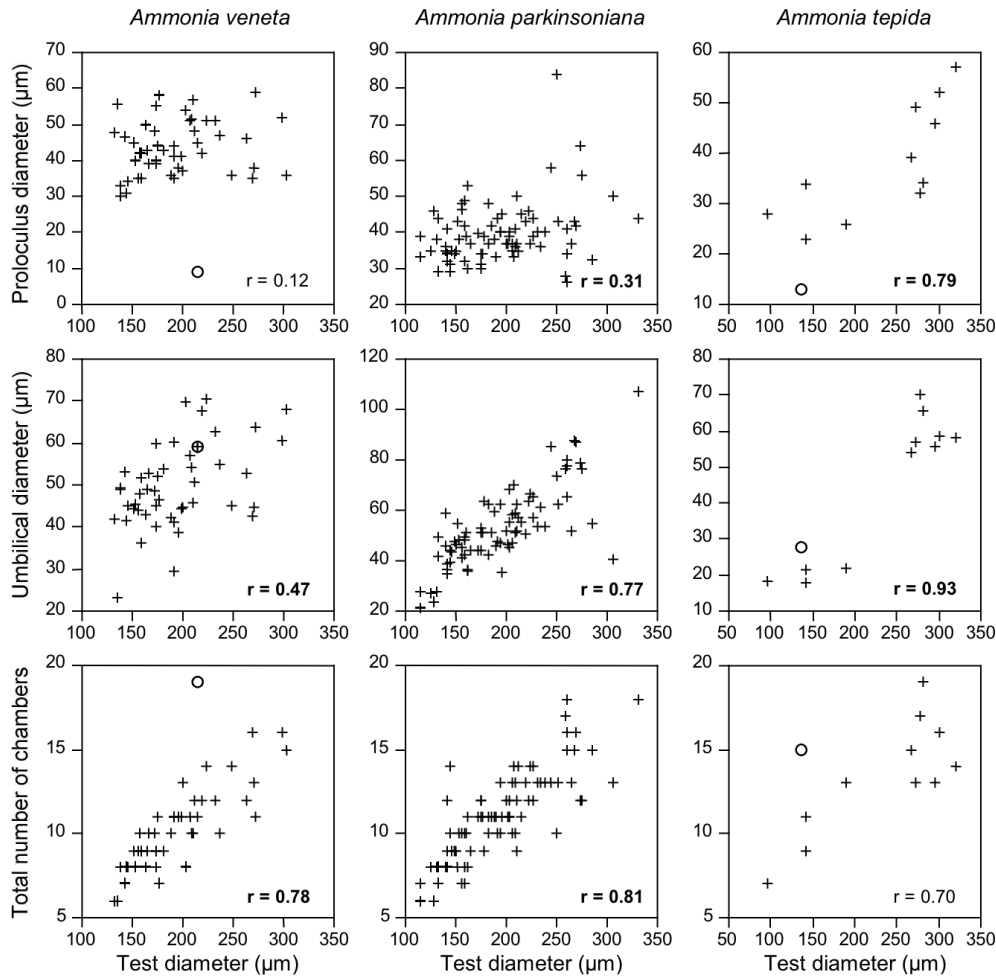


Figure 5. Correlation of proloculus and umbilical diameter, as well as the total number of chambers with the maximum test diameter of *A. veneta*, *A. parkinsoniana*, and *A. tepida*. Correlation coefficients with a 99 % significance level are highlighted in bold. Circles: microspheric specimens.

environmental variability (Langer et al., 1989; Seuront and Bouchet, 2015).

4.2 Constraints on a morphological species concept

Benthic foraminifera are investigated in biological and paleontological studies. Therefore, phenotypic differences of the fossil preservable test are to be used for species discernment (e.g. Benton and Pearson, 2001). At least one unique characteristic should discriminate a foraminiferal species from other taxa (Diagnosable Species Concept; Nixon and Wheeler, 1990; de Queiroz, 2007).

In the present study, sorting of specimens with similar morphologies was pursued in advance of species designation. Sorting involved intuitive pattern recognition, instant comparison of all specimens, and attempted an assemblage homogenization. A multitude of criteria were unconsciously applied by the observers, which were far beyond those listed in the original species descriptions. The vast ap-

plication of such specialist experience has often been criticized as it leads to an overenthusiastic splitting of taxa (Drooger, 1993), in particular when minute morphological details from SEM images were considered (Simmons and Bidgood, 2021). Instead of typological determinations, morphometric approaches were proposed to ensure a robust and reliable species identification, also by different independent examiners (Less and Kovács, 2009).

Indeed, we achieved a 100 % consensus on species determination in 53 % of the individuals and a 75 % consensus among four observers in 82 % of the specimens on average. The consensus rates did not improve during repetitions and with advancing practice. It therefore appears plausible that typological species determinations were found impracticable in the genus *Ammonia* due to its high morphological variability (Poag, 1978; Jorissen, 1988; Walton and Sloan, 1990). Consequently, genotypes were identified by phylogenetic cluster analyses of rDNA sequences and related to morphometric parameters to establish a robust morphologic

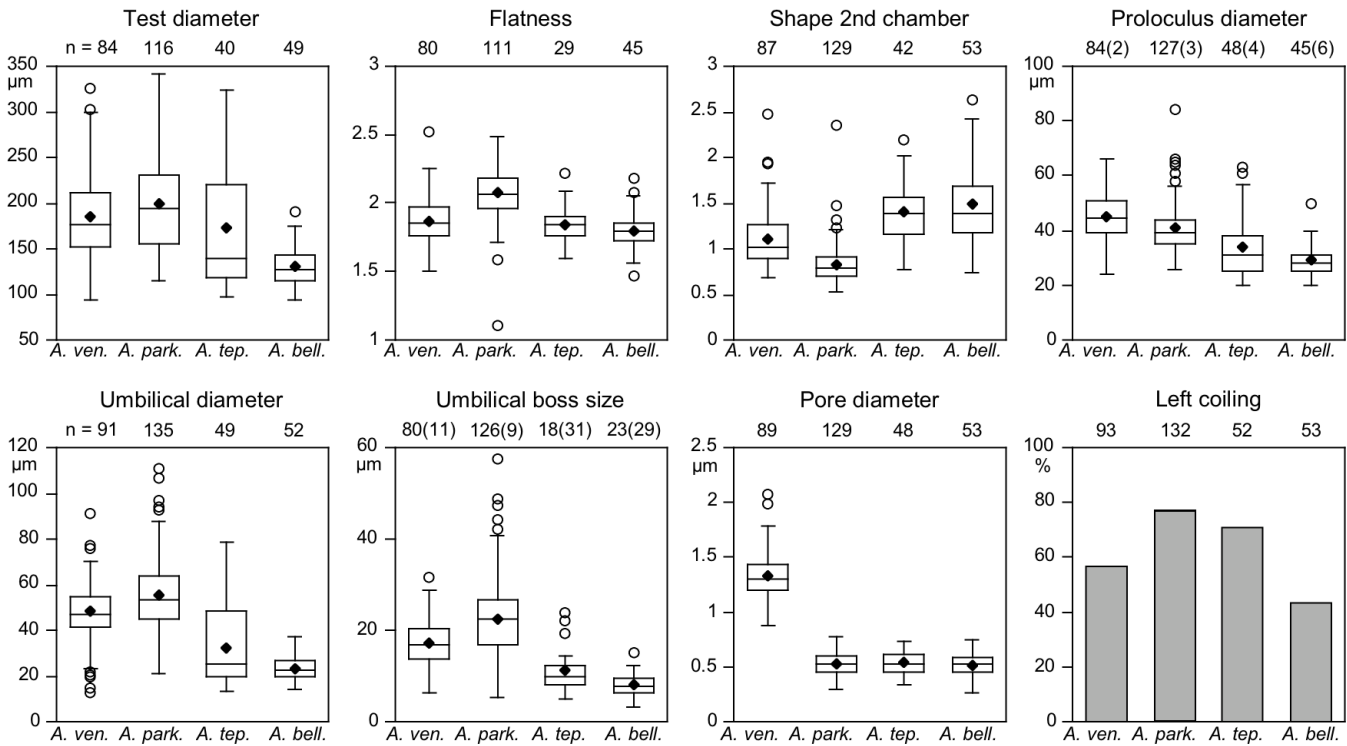


Figure 6. Mean values (diamonds) and frequency distribution of species-distinctive biometric parameters of *Ammonia* species considered in this study. The box plot displays $\pm 25\%$ of the data around the median value. The circles depict outliers for the range of 75% of the values around the median. Data from intact and damaged specimens were included. Numbers in brackets at the proloculus diameter indicate the counts of microsppheric specimens and specimens without an umbilical boss. Abbreviations: bell.: *bellaria*, park.: *parkinsoniana*, tep.: *tepada*, ven.: *veneta*.

designation and reliable discrimination of *Ammonia* species (Hayward et al., 2004). The assignments of morphologically determined species to genotypes were provided by Hayward et al. (2021, their table 2).

For instance, *Ammonia veneta* (genotype T1) is characterized, among others features, by a test diameter of up to 400 μm , 6.5 to 8 chambers in the last whorl, a pore diameter between 1.5 and 2.5 μm , sutural calcite ridges on the spiral side, and a relative length of the third radial sutural furrow on the umbilical side of 50% to 70% (Table B7). While the number of chambers and radial furrow length from the literature fit the range of values obtained in the present study, the living specimens from Bellaria are much smaller, their pore diameter is in the lower part of the above data range and far lower than those reported by Richirt et al. (2019), and thickened sutural ridges are developed in not more than 69% of our specimens from Bellaria. Flatness, dimensions of the second chamber, and proloculus size are also close to the lower limit of the range of values reported in the literature (Fig. 7).

The tests of *Ammonia parkinsoniana* (genotype T9) are up to 700 μm in diameter and have 8 to 13 chambers in the last whorl (Table B7), a circular, moderately large and flat umbilical boss, long and curved sutural furrows on the umbilical side, and folia that are often bluntly pointed. In our living

specimens from Bellaria, the diameter is far lower than the literature range; the number of chambers roughly fits with 6 to 11 in the last whorl, an umbilical boss is shown by 93% of the specimens, and only less than half of the sutures are curved on the umbilical side (Table B6). The other parameters are also in the lower range or far below the data range as reported in the literature (Fig. 7).

Ammonia tepida (genotype T20) shows, among other characteristics, a test diameter of up to 300 μm , 7 chambers in the last whorl, a lobulate peripheral outline, low sutural ridges on the spiral side, small pustules in the umbilical but no umbilical boss, and small pores of 0.3 to 0.9 μm diameter (Table B7). Despite the fact that this species is now considered to be endemic to the western Atlantic, Gulf of Mexico, and Caribbean, most of the parameters obtained in the present study fit the lower literature data range (Fig. 7). Only the flatness and the shape of the second chamber fit the data range of *Ammonia aberdoveyensis* (genotype T2) slightly better. The latter species is confined to the North Atlantic, North Sea, and Mediterranean. Furthermore, 63% of our specimens show an umbilical boss (Table B6). This feature should be absent from the genuine *Ammonia tepida* but is developed as one or several small knobs in the umbilicus of *Ammonia aberdoveyensis*. On the other hand, the mean number of cham-

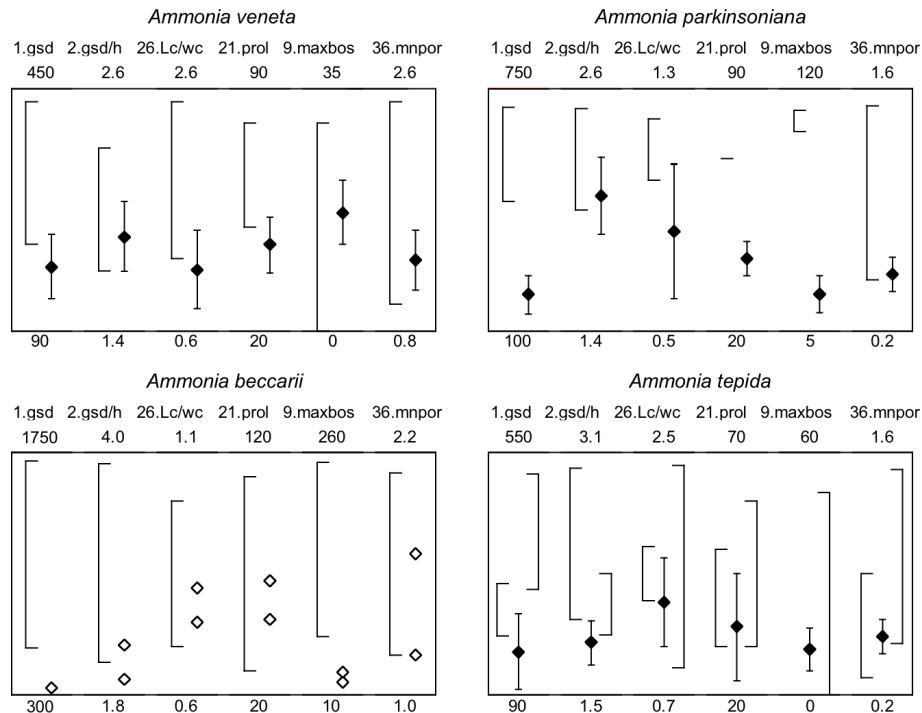


Figure 7. Maximum test diameter and ranges of five diagnostic biometric parameters of the three ranked species and dead *Ammonia beccarii* from Bellaria (see Table B2 for abbreviations). Diamonds and error bars indicate the mean value and standard deviation (1σ), and open diamonds are single measurements obtained in the present study. Brackets to the left depict the data range from the literature as reported by Hayward et al. (2004, 2019, 2021). Brackets to the right in the panel of *Ammonia tepida* depict the literature data range of *Ammonia aberdoveyensis*. Minimum and maximum y-axis limits are given on the bottom and top of the panels.

bers in the last whorl was 6.5 in the present study and thus fits *A. tepida* (6–8) much better than the *A. aberdoveyensis* (8–9) (Haynes, 1973). The lobulate peripheral outline of most of the juvenile specimens from Bellaria is in good agreement with locotypes of *A. tepida* as well. Unless genetic investigations assess the genotype affiliation of living specimens from Bellaria, we will keep with the denomination as *A. tepida* in its typological common use.

The biometric parameters of the two dead specimens of *Ammonia beccarii* also fit the lower range of the literature data (Table B7). They are far smaller than the ones reported in the literature (Fig. 7), including two presumably juvenile specimens figured by Haake (1977). Our specimens from Bellaria show, in addition, beads along the radial sutures (Table B6), which were also clearly visible in light microscopic images. This feature was not recognized in *Ammonia veneta* and thus may serve as a distinctive feature for juvenile or small individuals of *Ammonia beccarii*.

4.3 A retrospect to the 1850s

The earliest comprehensive work on foraminifera from the Adriatic Sea was published by Schultze (1854), including a review of the knowledge of these organisms as of the mid-19th century. Max Sigmund Schultze, a medical scientist

from Greifswald University, northern Germany, and founder of the cell theory in physiology, went on an expedition from August to October 1853 and took samples at the port of Trieste, in the adjacent Muggia Bay, and on a sand bank off Trieste. He could not recover living foraminifera from these locations. Sampling was successful on the sand bottom at the port of Ancona and further to the north up to a maximum depth of 20 ft (6.28 m; 1 ft in the Kingdom of Prussia was equal to 0.314 m). He also sampled a rocky shoal overgrown with algae at a few feet to intertidal depth to the south of Ancona port and muddy channels on the lagoonal side of Lido Island, Venice. Max Schultze also considered a sample from Rimini Beach that he received from Friedrich von Hagenow, Greifswald, and another mud sample from Muggia Bay that was sent to him in March 1854 by Heinrich Freyer, Trieste, together with Adriatic seawater for foraminiferal culturing.

Max Schultze used a linen mesh to scrape sediment from the surface. The maximum sampling depth of 6.28 m suggested that he could have fixed the mesh like a spoon net on the tip of a punting stake that is usually 4 to 6 m long. The samples were filled in glass beakers with seawater and stirred, and the suspension was decanted including algae and other organic debris. The samples were left for awhile under seawater, and the walls were inspected for foraminifera that had crawled upwards. The residue was also examined for

living foraminifera and gromids. Occasionally, a sieve with $0.1'''$ ($226\ \mu\text{m}$; unit $'''$ = French ligne, $1''' = 2.2558\ \text{mm}$) mesh size was used to concentrate foraminiferal tests from sand samples.

Schultze took the samples back to Greifswald where the foraminifera were still alive and active until July 1854. He kept them in glasses, observed foraminiferal motion, performed dissections and experiments, examined their cell structure, nuclei, and vacuoles, assessed chamber formation and calcification, and described 24 new taxa.

Basically, Schultze (1854) recorded three *Ammonia* species in Adriatic littoral to nearshore environments, which were assigned to the genus *Rotalia* at that time. *Rotalia veneta* and *Rotalia freyeri* were found living. *Rotalia beccarii* was retrieved as empty shells from the sand sample collected at Rimini by Friedrich von Hagenow. The assignment of *Ammonia veneta* to genotype T1 was based on a specimen from an intertidal mud patch at Torcello Island, Venice lagoon (Holzmann et al., 1998), which was established as a neotype and deposited at the Smithsonian Institution, Washington, DC (USNM PAL 770961) (Hayward et al., 2021). The test geometry and pore size as reported by Schultze (1854) were considered diagnostic characteristics, even though Richirt et al. (2019) found the crescent sutures on the umbilical side and the size of the reported specimens to be in disagreement with genotype T1. The biometric data from the present study, however, revealed that not only the pore diameter ($0.0005''' = 1.1\ \mu\text{m}$), but also the test diameter of large specimens ($0.16''' = 361\ \mu\text{m}$), largest and smallest proloculus diameter ($0.023''' = 52\ \mu\text{m}$; $0.016''' = 36\ \mu\text{m}$), and the number of chambers in the last whorl (7–8) is in good agreement with recent morphotypes from the Adriatic (Table B6). Schultze (1854) noted that the finer structure of the shell is very similar to *A. beccarii* (p. 59). This may be considered evidence for the recognition of raised calcite ridges on the sutures of *A. veneta*, even though he did not mention that explicitly.

Ammonia freyeri has scarcely been mentioned in the literature (e.g. Holzmann, 2000). This may be due to the fact that Schultze (1854) figured only the spiral side and an apertural aspect. The umbilical side was not described but characterized as being low convex. Considering the shape and geometry of the figured specimens, they appear to be very similar to *A. parkinsoniana*. Furthermore, Schultze mentioned clusters of irregular, low knobs along the sutures on the umbilical side of the last chambers and depicted them in fig. 6 on his Plate 3. Similar structures were only found in *A. parkinsoniana* in the present study (e.g. Fig. 8, nos. 6, 10). From a typological point of view and on the basis of the information provided, the species are the same. However, the pore diameter according to Schultze is $0.0008'''$ ($1.8\ \mu\text{m}$) and thus much higher than in *A. parkinsoniana* ($0.53 \pm 0.10\ \mu\text{m}$). Experimental evidence suggests that a doubling of the pore diameter may occur under dysoxic conditions (Moodley and Hess, 1992), whereas Schultze's specimens were col-

lected in well-ventilated environments. The total number of chambers of the above-mentioned specimen (22) is much higher and the proloculus diameter ($0.008''' = 18\ \mu\text{m}$) is much smaller than in *A. parkinsoniana* (total number of chambers $11.5 \pm 3.0\ \mu\text{m}$, proloculus diameter $41 \pm 8.4\ \mu\text{m}$) (Table B6) unless Schultze described a microspheric individual like specimen no. 234 of the present study (22 chambers, proloculus diameter $17\ \mu\text{m}$). Microspheres are, on the other hand, very rare in *A. parkinsoniana* (2%). The same applies to *A. beccarii*, for which Schultze reported a proloculus diameter of $0.007'''$ ($16\ \mu\text{m}$), whereas it is commonly in the range of 30 to 50 μm (Table B7).

These discrepancies raise the question of the optical precision of microscopes in the mid-19th century. Achromatic lenses were already invented, and they were close to the physical resolution of light microscopy. Test objects were available with calibrated resolutions of 0.4 to 0.6 μm (Turner, 1967). Friedrich Nobert at Greifswald manufactured reliable test plates with a resolution of 1.1 μm in the early 1850s, and eyepiece scales were developed and in use (Horst Kuhn and Alfons Renz, Tübingen, personal communication, 2021). It is therefore conceivable that microscopic equipment with a sufficient precision was readily available at Greifswald University and was used by Max Schultze.

Nonetheless, there were serious time constraints in his study. The report of Schultze's investigations was accomplished not later than 10 months after sampling. Some observations were made in June 1854, i.e. 1 month before closure, and the book was printed in the same year. A peer-review process was not yet established in the era of independent private scholars. As such, it is not to wonder why some details were not provided. Literal errors in copying measurement values from the laboratory journal to the paper are likely to have occurred and probably were not corrected. Samples, type specimens, and microscopic slides no longer exist in the collections at the universities of Greifswald and Bonn. Without physical evidence it is impossible to prove whether *A. freyeri* is indeed a junior synonym of *A. parkinsoniana*.

5 Conclusions

Five different *Ammonia* species were recorded in the living (rose-bengal-stained) fauna off Bellaria, Italy, at water depths of 0.5 to 3 m. *Ammonia parkinsoniana* and *A. veneta* were the most frequent species. One species was recorded for the first time and is denominated *Ammonia bellaria* n. sp. in the present study. *Ammonia beccarii* was found in the dead assemblage only. With reference to the recent distribution of this species in the northern Adriatic (Donnici and Barbero, 2002), the upper depth limit is now constrained to a water depth between 3 and 5 m. Small specimens like those we have found may well have been transported to shallower depths by wave action during storm events. Large specimens, like the neotype from Rimini Beach, were most likely ar-

tificially displaced from late Pleistocene deposits dredged in 40 m water and transported to the type locality by sand pumping during beach augmentation.

Ammonia species have commonly been established on large, adult tests as holotypes and brief descriptions emphasizing main characteristics and phenotypic differences to other taxa. The types of many species were lost. Therefore, typological determinations were prone to a high degree of subjectivity. Our procedures revealed that the determination of every other specimen is no matter of debate. Randomly, three of four observers agree upon four of five specimens. The same level of consensus emerged in recognition as simple as whether folia on the umbilical side were straight or curved. Six of 20 parameters, i.e. the flatness of the test, umbilical and proloculus diameter, the diameter of the largest umbilical boss, the proportions of length and height of the second chamber, and the mean pore diameter, were not substantially biased by subjectivity and could be used for morphometric species determination.

Ontogenetic influences on biometric parameters were found to be of minor importance or almost not recognizable, even though some of them showed a statistically significant relationship with test size in the present study. There were, however, physiological and ecological factors that exert a certain influence on the biometry of *Ammonia* species. The proloculus diameter, i.e. size of juveniles produced during asexual reproduction, revealed that larger juveniles grow faster and are more competitive in food acquisition. The increase in flatness and convexity with growth in *A. veneta* and *A. parkinsoniana* ensures a good responsiveness of the individuals to environmental stimuli during all ontogenetic stages.

In a comprehensive approach, the biometry of all specimens from the living fauna was assessed. The biometric data on the above-mentioned species-distinctive parameters showed high intraspecific variability. The frequency distributions were often very similar among species. Some parameters, however, were distinctively different: for instance, the flatness and shape of the second chamber of *A. parkinsoniana*, the pore diameter of *A. veneta*, and the umbilical diameter of *A. bellaria*. The proportion of microspheres and dextral coiled specimens is also higher in this species. In combination, the averages of these biometric values are considered suitable for species discrimination. However, the values from the living fauna from offshore of Bellaria were mostly at the lower limit or far below the data range reported in the literature. We consider this to be an artificial bias because the latter are based on measurements from a few adult specimens from the dead assemblage and not from the entire living fauna as in the present study. Nonetheless, our biometric approach was not successful in a secure discrimination of *A. aberdoveyensis* and *A. tepida*. Our results furthermore indicate that the presence of beads along the sutures on the umbilical side of *A. beccarii* is a distinctive characteristic to discriminate younger specimens from adults of *A. veneta* with the same

size. This sheds light on the high proportions of *A. beccarii* in the northern Adriatic as reported in the literature, which therefore may well be a result of lumping these two species.

In essence, the application of biometric parameters in combination with the consideration of qualitative characteristics facilitates a robust identification of *Ammonia* species without genetic analyses. This approach is also applicable to earlier literature data, even from the mid-19th century. Their re-assessment is critical for a correct denomination of recent species and genotypes.

Appendix A: Taxonomy

Following Hayward et al. (2021), the suprageneric foraminiferal classification as proposed by Pawlowski et al. (2013) and Holzmann and Pawlowski (2017) has been applied. For the *Ammonia* species discussed in this paper, extended lists of synonymies were provided by Hayward et al. (2021). We therefore referred to the type description, selected papers on foraminifera from the Adriatic Sea, and Hayward et al. (2021). References to images in this paper are given in square brackets.

Phylum FORAMINIFERA d'Orbigny 1826

Class GLOBOTHALAMEA Pawlowski et al. 2013

Order ROTALIIDA Delage and Hérouard 1896

Superfamily ROTALIOIDEA Ehrenberg 1839

Family AMMONIIDAE Saidova 1981

Genus *Ammonia* Brünnich, 1771

Ammonia beccarii (Linné 1758)

[Fig. 12, nos. 1-3]

Nautilus beccarii Linné, 1758, p. 710.

Ammonia beccarii (Linné), Mouanga, 2017, pl. 16, figs. 1a–c

Ammonia beccarii forma *beccarii* (Linné), Jorissen 1988, pl. 5, figs. 1–4

Ammonia beccarii (Linnaeus), Cimerman and Langer, 1991, p. 76, pl. 87, figs. 3–4

Ammonia papillosa (d'Orbigny), Morigi et al., 2005, pl. 1, figs. 4a–b.

Ammonia beccarii, Serandrei Barbero et al., 2008, pl. 33.

Ammonia beccarii (Linné 1758), Hayward et al., 2021, 153–154, pl. 17, figs. 7–12; pl. 18, figs. 7–12; pl. 19, figs. 5–10; text-fig. 31.

Description

The test is very low-trochospiral and biconvex. The peripheral margin is subacute and keeled, and the profile is compact and circular. The test consists of 3.5 to 4 whorls, with up to 14

chambers in the last whorl. The chambers are trapezoidal to subrectangular on the spiral side and triangularly elongated on the umbilical side. The sutures on the spiral side are raised and slightly curved; in the earlier part of the test they are characterized by the typical transverse pustules and ridges, becoming less marked in the last whorl. They are straight on the umbilical side and also characterized by transverse pustules and ridges. The umbilicus is moderately large and presents a large knob, especially in late ontogenic stages. In younger specimens, there may be several smaller knobs. The aperture is an interiomarginal slit. The wall texture is smooth and the pores are small.

Distinguishing features

The numerous chambers in the last whorl, the compact profile, the strongly triangular chambers on the umbilical side, the aperture consisting of an interiomarginal slit, and the marked transverse pustules and ridges are considered diagnostic features of this species. In particular, *A. beccarii* differs from *A. parkinsoniana* by its more numerous chambers in the last whorl of adult specimens, its lower trochospire, and its strong ornamentations consisting of transverse pustules and ridges. It differs from *A. bellaria* by its more compact peripheral margin, its well-developed keel, more numerous chambers in the last whorl, and its transverse pustules and ridges on both sides. It differs from *A. tepida* by its larger test, its more compact and non-lobate profile, the keeled peripheral margin, and the more numerous chambers in the last whorl.

Dimensions

Hayward et al. (2021) reported that adult specimens are generally very large, up to 1700 µm in diameter. Our intact specimen from Bellaria is much smaller with 344 µm diameter. The mean pore diameter is 1.4 µm.

Remarks

In the material from Bellaria, specimens similar to the large morphotypes described by Hayward et al. (2021) have not been found either alive or in the dead assemblages.

Ammonia parkinsoniana (d'Orbigny 1839)

[Fig. 8, nos. 1–16, Fig. 12, no. 7]

Rosalina parkinsoniana d'Orbigny 1839, p. 99, pl. 4, figs. 25–27.

? *Rotalia freyeri* Schultze 1854, p. 59, pl. 3, figs. 6, 7.

Ammonia parkinsoniana (d'Orbigny) forma *parkinsoniana*, Jorissen, 1988, p. 46, pl. 9, figs. 1–5.

Ammonia parkinsoniana (d'Orbigny), Cimerman and Langer, 1991, p. 76, pl. 87, fig. 9.

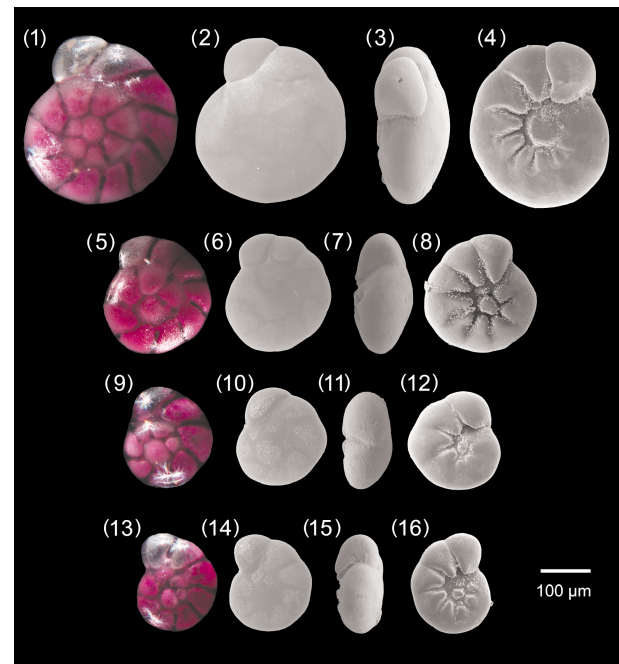


Figure A1. *Ammonia parkinsoniana*. 1–4: specimen no. 194, 5–8: specimen no. 423, 9–12: specimen no. 198, 13–16: specimen no. 200.

Ammonia parkinsoniana (d'Orbigny), Mouanga, 2017, p. 226, pl. 16, figs. 3a–c.

Ammonia parkinsoniana (d'Orbigny), Hayward et al. 2021, p. 180, pl. 14, figs. 12–14, pl. 15, figs. 12–14, pl. 16, figs. 12–13, text-fig. 64.

Description

The test is low-trochospiral, the profile is generally biconvex, and the spiral side is general slightly more convex spiral. The peripheral margin is broadly rounded. The test is composed of around 4 whorls; the final whorl comprises 8–10 chambers, and the last 1 to 3 may be inflated. The shape of the chambers is oblique trapezoid on the spiral side and triangular on the umbilical side. The sutures on the spiral side spiral are slightly depressed, oblique, and may be curved backwards. In the earlier part of the test, the sutures on the spiral side are slightly depressed and may be curved backward to become straight, sometimes thickened, and may be elevated in the last whorl. On the umbilical side, the sutures are depressed, slightly curved, and very depressed towards the umbilicus. The inner part of the depressions is covered by small, conical pustules with varying density. The triangular ending of the chambers on the umbilical side pointing to the umbilicus may be thickened and indistinctly raised. A large and sometimes flatted knob is present in the umbilicus of most specimens; it may be missing or replaced by a few small pustules in juvenile specimens. The aperture is a narrow umbilical–extraumbilical slit extending into the moder-

ately wide umbilicus. The wall texture is smooth, with small and indistinct the pores.

Distinguishing features

A. parkinsoniana differs from *A. bellaria* by its less lobate profile, rounded peripheral margin, and the presence of a larger knob in adult specimens. It differs from *A. veneta* by its smoother sutures on the spiral side, its large knob in the umbilical area, and the smaller and indistinct pores. *Ammonia parkinsoniana* differs from *A. tepida* by its more numerous chambers in the last whorl, its less lobate profile, and the presence of the large knob in the umbilicus of adult specimens.

Dimensions

The size range of *A. parkinsoniana* in the fauna from Bellaria is 115–342 µm, the mean pore diameter is 0.53 µm (± 0.10 µm, 1σ), and the mean diameter of the umbilical boss is 22.5 µm (± 8.6 µm, 1σ).

Remarks

In the original description and drawing of d'Orbigny (1939), *A. parkinsoniana* shows much more strongly curved and retroflex sutures on both sides and a flatter test than in the specimens found in this investigation.

Images with a strongly planoconvex profile are often reported in the literature (see Cimerman and Langer, 1991, pl. 87, fig. 9) compared to the type figure of d'Orbigny (1939). The large umbilical boss is considered a distinctive characteristic of this species.

Ammonia veneta (Schultze 1854)

[Fig. 9, nos. 1–16, Fig. 12, nos. 1–3, 8]

Rotalia veneta Schultze 1854, p. 59, pl. 3, figs. 1–5.

Ammonia parkinsoniana (d'Orbigny) forma *tepida*, morphotype 4, Jorissen, 1988, p. 60, pl. 10, figs. 2, 3.

Ammonia beccarii (Linné), von Daniels, 1970, pl. 7 figs. 5a–c.

Ammonia sp. 1, Cimerman and Langer, 1991, p. 77, pl. 88, figs. 1–4.

Ammonia sp. 1, Mouanga, 2017, p. 227, pl. 16, figs. 5a–c.

Ammonia veneta (Schultze), Hayward et al., 2021, p. 192, pl. 11, figs. 1–4, pl. 12, figs. 1–4; pl. 13, figs. 1–3; pl. 27, figs. 28–30; pl. 33, figs. 1–3, text-fig. 77.

Description

The test is trochospiral and biconvex. The peripheral margin is broadly rounded and the outline slightly lobate. The test is composed of 2–3 whorls with 6 to 8 chambers in the last

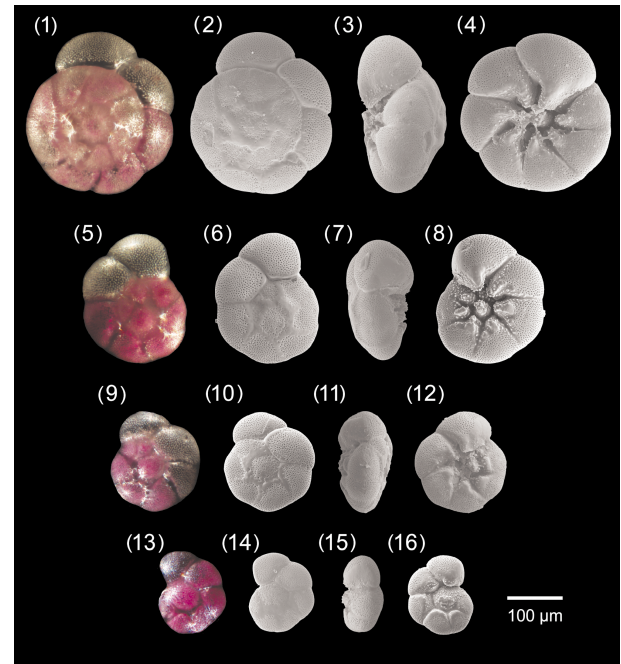


Figure A2. *Ammonia veneta*. 1–4: specimen no. 55, 5–8: specimen no. 105, 9–12: specimen no. 309, 13–16: specimen no. 212.

whorl. On the spiral side the chambers are trapezoidal to sub-rectangular, whereas they are subtriangular on the umbilical side. The last two or three chambers may be slightly more inflated than the previous ones, and the spiral suture separating them may be slightly depressed. In general, sutures of the earlier chambers in the inner whorls are oblique, raised, and covered by calcite ridges on the spiral side. On the umbilical side the sutures of earlier chambers are curved, flush on the outer side, and open to deep openings close to the umbilicus. They are covered by small pustules in the inner side. The umbilical extension of each triangular chambers is curved backwards, tapering, and thickened. They may rise to elevated papillae. Usually, one to three knobs are present in the moderately wide umbilical area; they are also covered by small pustules. The aperture is an umbilical–extraumbilical arch that extends into the umbilicus, where it may be bounded by a narrow flap. The wall texture is coarsely perforated compared to other *Ammonia* species.

Distinguishing features

The thickened and raised sutures on the spiral side, the markedly coarse pores, and papillae on the umbilical extensions of earlier chambers on the umbilical side distinguish this taxon from other *Ammonia* species in the study area.

Dimensions

The size range of *A. veneta* at Bellaria is 94–326 µm, and the mean pore diameter is 1.33 µm (± 0.22 µm, 1σ).

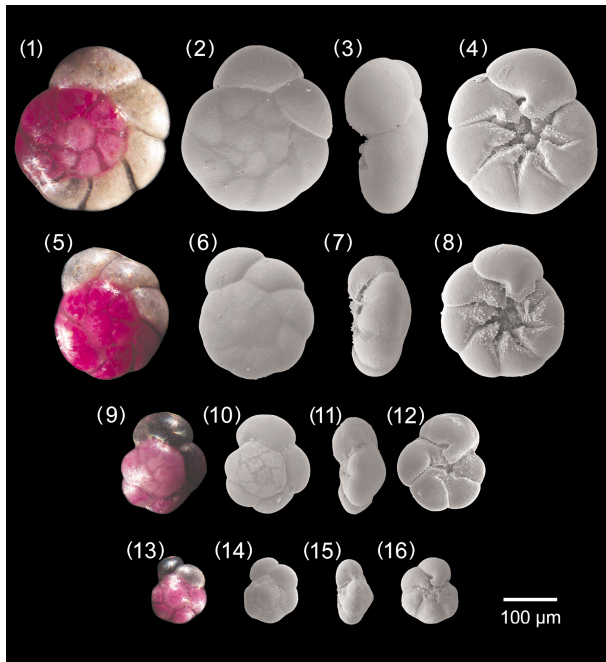


Figure A3. *Ammonia tepida*. 1–4: specimen no. 128, 5–8: specimen no. 129, 9–12: specimen no. 186, 13–16: specimen no. 322.

Remarks

Our specimens from the Bellaria region resemble *Ammonia parkinsoniana* forma *tepida* morphotype 4 of Jorissen (1988) and *Ammonia* sp. 1 of Mouanga (2017). Schultze (1854) described specimens of this species from muddy sediments retrieved from the Venice lagoon. They were rare in channels on the lagoonal side of Lido island and very rare in muds from the Bay of Muggia, Trieste. Surprisingly, this species has not been documented in later papers on foraminifera from Venice lagoon (e.g. Donnici et al., 1997; Donnici and Serrandrei-Barbero, 2002) or anywhere else in the Adriatic Sea. *Ammonia?* *veneta* as figured in the southwestern Atlantic by Boltovskoy et al. (1980, pl. 35, figs. 1–3) is more reasonably *Aubignyna perlucida*. *Ammonia veneta* is attributed to phylotype T1 (e.g. Hayward et al., 2021). The umbilical characteristic of an *Ammonia* specimen from Playa Bailén, Cuba (Cuba-642), representing the molecular type T1 is very similar to the drawings of *A. veneta* type specimens, whereas the spiral side is different (Hayward et al., 2004).

Ammonia tepida Cushman 1926

[Fig. 10, nos. 1–16, Fig. 12, nos. 4–6, 9]

Rotalia beccarii var. *tepida* Cushman 1926, p. 79, pl. 1.

Ammonia parkinsoniana (d’Orbigny) forma *tepida*, Jorissen, 1988, p. 58, pl. 7, figs. 1–4.

Ammonia tepida (Cushman), Cimerman and Langer, 1991, p. 76, pl. 87, figs. 10–12.

Ammonia tepida (Cushman), Mouanga, 2017, p. 227, pl. 16, figs. 4a–c.

Ammonia tepida (Cushman), Hayward et al., 2021, p. 188, pl. 8, figs. 9–10, pl. 9, figs. 9–10, pl. 10, figs. 9–10, text-fig. 73.

Description

The test is trochospiral and almost equally biconvex, and the spiral side is slightly more convex than the umbilical side. The peripheral margin is rounded and the profile is markedly lobate. The test consists of 2.5 to 3 whorls, with 5 to 8 inflated, almost globular chambers in the last whorl. The chambers are trapezoidal on the spiral side and triangular on the umbilical side. The sutures of the final whorl may be raised in the earlier part of the test. They are straight on the spiral side but oblique and slightly curved on the umbilical side.

Close to the umbilical area sutures are more depressed and wider, open into angular open spaces, and are characterized by fine pustules more densely concentrated on their borders. A well-marked notch sensu Hottinger (2006) is visible on the sutures separating the chambers in the umbilical area near the umbilicus. It can be also defined as an umbilical folium with a protoforamen; folia can be also covered by pustules. Adult specimens can be characterized by more or less developed plugs in the umbilicus, which is open and moderately wide. The aperture is an umbilical–extraumbilical low arch. The wall texture is smooth and the pores are very small.

Distinguishing features

The few chambers in the last whorl, the very lobate profile, the umbilical folia with protoforamina, and the angular space between sutures are considered diagnostic features of this species. In particular, *A. tepida* differs from *A. parkinsoniana* by its very lobate profile, less numerous chambers in the last whorl, the notch on the sutures close to umbilical area, and the absence of the large knob in the umbilicus. It differs from *A. bellaria* by its rounded peripheral margin and by the presence of the angular space between the sutures. It differs from *A. veneta* by its smooth sutures on the spiral side, less numerous chambers on the spiral side, and its smaller pores.

Dimensions

Cushman (1926) reports that the maximum diameter of this species never exceeded 0.35 mm. The size range of *A. tepida* from Bellaria is 97–324 µm, and the mean pore diameter is 0.54 µm (± 0.10 µm, 1σ).

Remarks

Hayward et al. (2021) showed the geographic distribution of *A. tepida* as restricted to the South Atlantic (Brazil and Caribbean), USA (Louisiana and Mississippi), and North

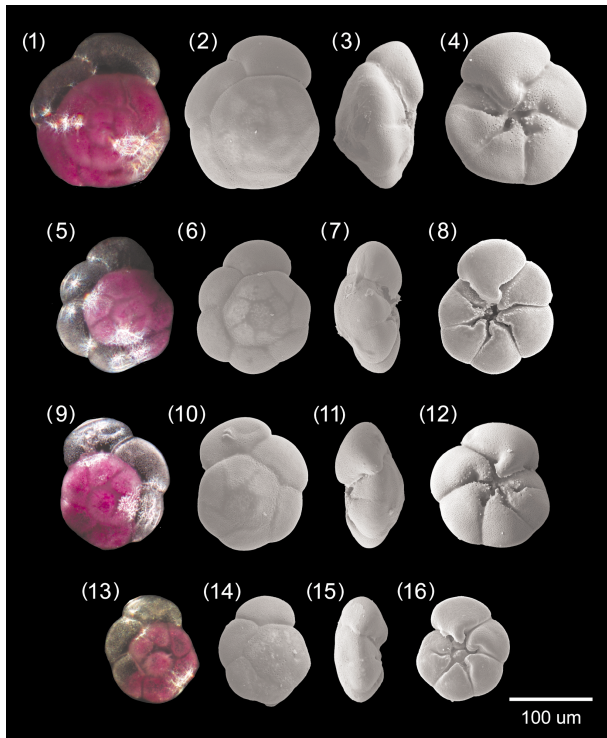


Figure A4. *Ammonia bellaria* n. sp. 1–4: specimen no. 174, 5–8: specimen no. 196 (holotype), 9–12: specimen no. 445, 13–16: specimen no. 71 (paratype).

Atlantic (Bermuda). However, our finding allows us to re-extend its occurrence to the Adriatic Sea in the Mediterranean Sea. Recently, the new genotype T20 has been assigned to this morphospecies (Hayward et al., 2021).

Ammonia bellaria n. sp.

[Fig. 11, nos. 1–16, Fig. 12, no. 10]

(ZooBank registration: the Life Science Identifier (LSID) for this article and the new species is urn:lsid:zoobank.org:act:14A03FD1-F303-4CFF-93CF-0E1CA866E126, registered on 15 November 2021, 10:30:25.130.)

Derivation of the name

From the town of Bellaria–Igea Marina at the Adriatic coast of Italy.

Diagnosis

A small, low-trochospiral, biconvex *Ammonia* with a smooth test, a lobate outline, a subacute peripheral margin, and a narrow umbilicus with a single small knob.

Holotype

Specimen no. 196 [Fig. 10, nos. 5–8], collection no. C39355.

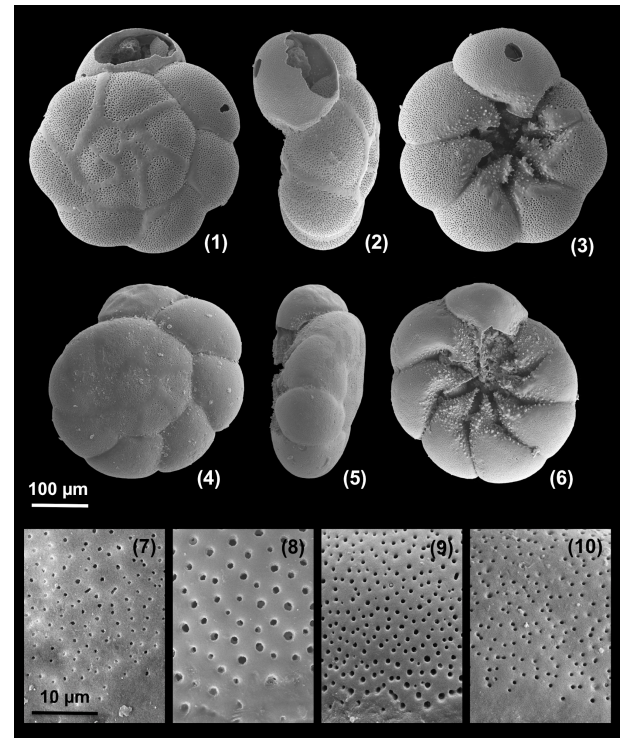


Figure A5. Large, dead specimens. 1–3: *Ammonia veneta* (specimen d2), 4–6: *Ammonia tepida* (specimen d7). Pores at the base of the second chamber. 7: *Ammonia parkinsoniana* (specimen no. 200), 8: *Ammonia veneta* (specimen no. 212), 9: *Ammonia tepida* (specimen no. 322) 10: *Ammonia bellaria* n. sp. (specimen no. 71, paratype).

Paratype

Specimen no. 71 [Fig. 10, nos. 13–16, Fig. 12, no. 10], collection no. C39356.

Material

56 living (rose-bengal-stained) specimens from Stations 1–4.

Repository

National History Museum, Basel.

Type locality

The landward side of a breakwater off the beach of Bellaria, north of the harbour (holotype: 44°8.824' N, 12°28.214' E, 0.8 m water depth; paratype: 44°8.787' N, 12°28.253' E, 2 m water depth).

Description

The test is low-trochospiral and biconvex. The peripheral margin is subrounded tending to subacute, and the profile is lobate. The test is composed of about three whorls, with

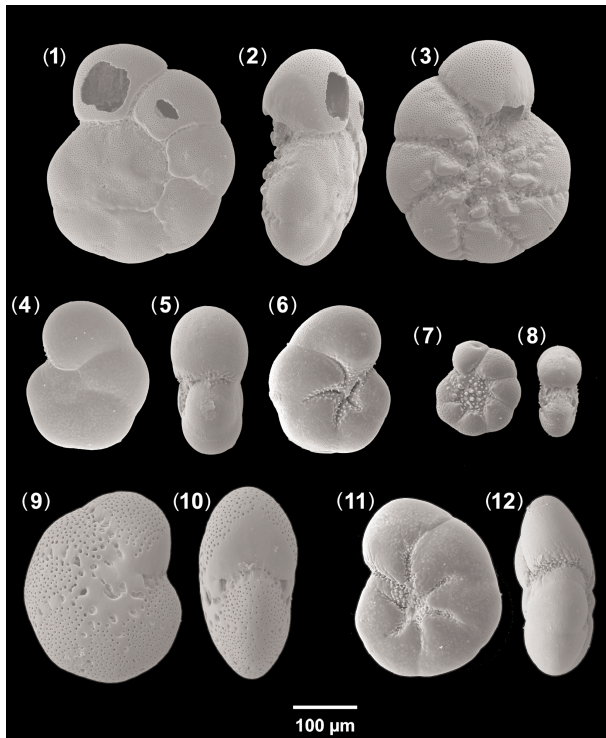


Figure A6. Accompanying fauna. 1–3: *Ammonia beccarii* (specimen d3), 4–6: *Aubignyna perlucida* (specimen no. 213), 7–8: *Haynesina depressula* (specimen no. 125), 9–10: *Elphidium translucens* (specimen d9), 11–12: *Haynesina germanica* (specimen no. 209).

five to seven chambers in the last whorl. Chambers are trapezoidal on the spiral side and triangular on the umbilical side. The termination of the chambers on the umbilical side tapers to extensions into the umbilical area and tends to turn backwards.

The sutures are straight to slightly curved, depressed, and not perforated on the spiral side. They are strongly depressed and slightly curved or retroflexed on the umbilical side. They are more incised toward the centre of the umbilicus, becoming less depressed towards the periphery.

A notch *sensu* Hottinger (2006) is visible on the sutures separating the chambers in the umbilical area near the umbilicus. It can also be defined as an umbilical folium with a small protoforamen. The umbilical area is moderately wide, incised, and characterized by small pustules concentrated on a small knob, which is not visible in side view. The knob may be absent in some specimens. The aperture is an umbilical–extraumbilical arched slit. The wall texture is smooth with small pores.

Distinguishing features

A. bellaria n. sp. differs from *Aubignyna perlucida* by its biconvex profile, the rosette-like chamber arrangement on the spiral side, and slightly larger pores. It differs from *A. parkin-*

soniana by its subacute peripheral margin, the smaller knob only visible on the umbilical side, the few pustules in the umbilical area, and less numerous chambers on the last whorl. It differs from *A. tepida* by its subacute peripheral margin and a less lobate profile. It differs from *A. veneta* by its biconvex profile, subacute peripheral margin, smaller pores, the presence of the small knob in the umbilical area, the less marked sutures on the spiral side, and less numerous chambers on the last whorl. It differs from *A. beccarii* by its biconvex profile, subacute peripheral margin, absence of transverse ridges and pustules on both sides, and smoother sutures. The umbilical area of *A. bellaria* n. sp. is the smaller observed in the *Ammonia* species investigated in this study.

Dimensions

Maximum diameter 167 μm (holotype) and 131 μm (paratype), size range of the fauna from the type locality 95–190 μm , mean pore diameter 0.51 μm ($\pm 0.09 \mu\text{m}$, 1σ).

Remarks

Other species mentioned in the paper

Ammonia aberdoveyensis Haynes, 1973, p. 184, fig. 38, nos. 1–7, pl. 18, fig. 15.

Ammonia beccarii (Linné) – *Nautilus beccarii* Linné, 1758, p. 710, pl. 1, fig. 1, pl. 19, figs. h, i [Fig. 13, nos. 1–3].

Ammonia falsobeccarii (Rouvilleis) – *Pseudoepionides falsobeccarii* Rouvilleis, 1974, p. 4, pl. 1, figs. 1–12.

Aubignyna perlucida (Heron-Allen and Earland) – *Rotalia perlucida* Heron-Allen and Earland, 1913, p. 139, pl. 13, figs. 7–9 [Fig. 13, nos. 4–6].

Elphidium translucens Natland, 1938, p. 144, pl. 5, figs. 3, 4 [Fig. 13, nos. 9, 10].

Haynesina depressula (Walker and Jacob) – *Nautilus depressulus* Walker and Jacob, 1798, p. 641, pl. 14, fig. 33 [Fig. 13, nos. 7, 8].

Haynesina germanica (Ehrenberg) – *Nonionina germanica* Ehrenberg 1840, p. 23 (figured in Ehrenberg, 1841, pl. 2, figs. 1a–g) [Fig. 13, nos. 11, 12].

Appendix B: Tables

Table B1. Station coordinates and water depth.

Station	Latitude	Longitude	Depth (m)
1	44°8.787' N	12°28.253' E	2
2	44°8.824' N	12°28.214' E	0.8
3	44°8.838' N	12°28.255' E	3
4	44°8.780' N	12°28.196' E	0.5

Table B2. Biometric parameters measured and assessed from SEM and light microscopic images of *Ammonia* specimens from Bellaria (Fig. 14). SEM: scanning electron microscope, LM: light microscope, sp: spiral side, um: umbilical side, av: apertural view. Code abbreviations after Hayward et al. (2004).

Parameter	measured on	Code
Maximum test diameter	SEM, sp ^a	1. gsd
Flatness (test diameter/height) ^c	SEM, av ^b	2. gsd/h
Convexity (high spiral side/high umbilical side)	SEM, av ^b	3. hs/lu
Diameter of the umbilicus between the ends of folia ^c	SEM, um	7. du
Relative length of 3rd radial sutural furrow on the umbilical side	SEM, um	8. rfl/w
Average diameter of the largest umbilical boss ^c	SEM, um	9. maxbos
Number of umbilical bosses	SEM, um	11. nobos
Calcite ridges or knobs on folia (yes/weak/none)	SEM, um	13. thckfol
Pustules on folia (yes/no)	SEM, um	14. folpust
Curved or straight folia (C/S)	SEM, um	17. pntfol
Beads along the edge of radial sutures (yes/no; dead specimens only)	SEM, um	18. radbd
Proloculus diameter ^c	LM, sp.	21. prol
Number of chambers in the last whorl	LM, sp.	22. chwh1
Total number of chambers including the proloculus	LM, sp.	25. ch
Shape or relative proportions of the 2nd chamber (length/height) ^c	SEM, sp.	26. Lc/wc
Smooth outline (% of 360°)	LM, sp.	27. perout
Spiral fissure length, if present (% of 360°)	SEM, sp.	28. spfis
Angle between the spiral suture and the radial suture between chambers 2 and 3 (°)	SEM, sp.	29. rad [^]
Raised calcite ridges on sutures of the spiral side (yes/no)	SEM, sp.	33. thckrad
Mean pore diameter on the spiral side of the 2nd chamber (mean of 13 pores on a line parallel to the base of the chamber) ^c	SEM, sp.	36. mnpor
Coiling direction on the spiral side (left/right) ^c	LM, sp.	Coiling direction
Microspheric specimen (yes/no) ^c	LM, sp.	Microspheric

^a Measurements were performed with LM and SEM. ^b Measurements were only considered when gsd could be measured on SEM. ^c Parameter considered for species discrimination.

Table B3. Living *Ammonia* species census data.

	Station 1	Station 2	Station 3	Station 4
<i>Ammonia veneta</i>	48	18	35	
<i>Ammonia parkinsoniana</i>	66	27	52	18
<i>Ammonia tepida</i>	30	7	18	3
<i>Ammonia bellaria</i> n. sp.	15	8	31	2
<i>Ammonia falsobeccarii</i>				1
indet. sp.	5	2	7	
Total	164	62	143	24
Standing stock (no. per 10 cm ³)	82	31	71.5	12

Table B4. Results of non-parametric Wilcoxon Mann–Whitney tests. Bold coefficients: p values ≤ 0.05 indicate that the compared data populations were significantly different with a 95 % confidence level (see Table B2 for abbreviations of biometric parameters).

(a) Intact vs. broken specimens						
	<i>A. veneta</i>	<i>A. parkinsoniana</i>				
7. du	0.25	0.05				
9. maxbos	0.29	0.02				
21. prol	0.15	0.02				
26. Lc/wc	0.79	0.59				
28. spfis	0.73	0.39				
36. mnpor	0.08	0.99				
(b) <i>A. veneta</i> populations at different stations						
	Stat. 1 vs. 2	Stat. 1 vs. 3	Stat. 2 vs. 3			
1. gsd	0.04	0.003	0.86			
7. du	0.64	0.57	0.59			
21. prol	0.28	0.65	0.73			
36. mnpor	0.86	0.89	0.83			
(c) <i>A. parkinsoniana</i> populations at different stations						
	Stat.1 vs. 2	Stat.1 vs. 3	Stat.1 vs. 4	Stat.2 vs. 3	Stat.2 vs. 4	Stat.3 vs. 4
1. gsd	0.56	0.0004	0.004	0.002	0.09	0.0002
7. du	0.83	0.01	0.01	0.06	0.05	0.0004
21. prol	0.82	0.09	0.01	0.25	0.06	0.01
36. mnpor	0.34	0.89	0.89	0.34	0.76	0.99

Table B5. Correlation of the maximum test diameter with other numerical biometric parameters of *Ammonia* species (see Table B2 for abbreviations). Only the intact specimens were considered for which all parameters could be measured. *r*: Pearson correlation coefficient, *p*: *p* value, *n*: number of values. Bold coefficients: *p* values ≤ 0.01 indicate a significance of >99% for this correlation.

1. gsd vs.	<i>A. veneta</i>			<i>A. parkinsoniana</i>			<i>A. tepida</i>			<i>A. bellaria</i> n. sp.		
	<i>r</i>	<i>p</i>	<i>n</i>	<i>r</i>	<i>p</i>	<i>n</i>	<i>r</i>	<i>p</i>	<i>n</i>	<i>r</i>	<i>p</i>	<i>n</i>
2. gsd/h	-0.12	0.429	48	0.40	0.000	80	0.46	0.136	12	-0.32	0.212	17
3. hs/hu	0.41	0.003	48	-0.09	0.421	80	-0.24	0.458	12	0.44	0.078	17
7. du	0.47	0.001	48	0.77	0.000	80	0.93	0.000	12	0.31	0.224	17
8. rfl/w	-0.13	0.379	48	-0.07	0.558	80	0.31	0.331	12	-0.02	0.928	17
9. maxbos	-0.02	0.920	44	0.71	0.000	75	0.61	0.196	6	-0.05	0.893	9
11. nobos	-0.28	0.058	48	0.18	0.101	80	0.20	0.535	12	-0.07	0.777	17
21. prol	0.12	0.434	48	0.31	0.006	80	0.79	0.002	12	0.27	0.291	17
22. chwh1	0.39	0.007	48	0.69	0.000	80	0.69	0.013	12	-0.25	0.342	17
25. ch	0.78	0.000	48	0.81	0.000	80	0.70	0.012	12	0.36	0.158	17
26. Lc/wc	0.47	0.001	48	-0.15	0.186	80	-0.36	0.255	12	0.64	0.006	17
27. perout	0.36	0.011	48	0.14	0.217	80	0.64	0.025	12	-0.04	0.868	17
28. spfis	0.51	0.001	38	-0.53	0.113	10	-0.60	0.290	5	0.41	0.214	11
29. rad [∧]	0.01	0.927	48	-0.27	0.015	80	-0.41	0.187	12	0.17	0.511	17
36. mnpor	0.59	0.000	48	-0.01	0.917	80	0.35	0.258	12	-0.02	0.953	17

Table B6. Total numbers, ranges, mean values, and standard deviations of biometric parameters measured and assessed for *Ammonia* specimens from Stations 1 to 3. Code abbreviations are given in Table B2. All distance measurements are given in micrometres (µm).

(a) <i>Ammonia veneta</i>					
48 intact, 52 not completely measured specimens					
	<i>n</i>	Minimum	Maximum	Mean	1σ
1. gsd	84	93.70	325.54	186.01	47.05
2. gsd/h	80	1.503	2.516	1.869	0.171
3. hs/hu	80	0.705	1.956	1.213	0.273
7. du	91	12.46	91.60	48.06	13.51
8. rfl/w	90	0.54	1.00	0.76	0.10
9. maxbos	80	6.28	31.53	17.19	4.54
21. prol (micro)	2	9	16	13	4.9
21. prol (mega)	84	24	66	45	8.1
22. chwh1	83	4	9	7.1	0.7
25. ch	80	4	22	10.2	2.9
26. Lc/wc	87	0.68	2.47	1.11	0.32
27. perout	77	0	100.0	71.0	22.7
28. spfis	68	8.4	46.2	23.6	9.5
29. rad [∧]	88	70.2	108.2	92.2	8.4
36. mnpor	89	0.88	2.07	1.33	0.22
11. nobos	14 = 0, 76 = 1, 3 = 2, 1 = 3 umbonal bosses				
13. thckfol	45 = yes, 24 = weak, 24 = none				
14. folpust	94 = yes, 1 = none				
17. pntfol	58 = curved, 37 = straight				
33. thckrad	63 = yes, 29 = none				
Coiling direction	40 = right, 53 = left				
Microspheric	2 = yes, 84 = none				

Table B6. Continued.

(b) <i>Ammonia parkinsoniana</i>					
81 intact, 57 not completely measured specimens					
	<i>n</i>	Minimum	Maximum	Mean	1 σ
1. gsd	116	115.14	341.69	198.64	51.91
2. gsd/h	111	1.101	2.480	2.072	0.192
3. hs/hu	111	0.703	1.866	1.100	0.207
7. du	135	21.23	110.69	55.41	16.73
8. rfl/w	132	0.47	0.97	0.70	0.11
9. maxbos	126	5.24	57.37	22.51	8.64
21. prol (micro)	3	10	17	14	3.5
21. prol (mega)	127	26	84	41	8.4
22. chwh1	127	6	11	7.9	1.0
25. ch	124	6	22	11.5	3.0
26. Lc/wc	129	0.53	2.35	0.83	0.22
27. perout	114	0	100.0	79.6	17.4
28. spfis	26	7.2	25.0	13.4	5.3
29. rad $\hat{}$	127	58.6	107.9	86.2	9.6
36. mnpor	129	0.29	0.77	0.53	0.10
11. nobos	10 = none, 113 = 1, 10 = 2, 2 = 3 umbonal bosses				
13. thckfol	11 = yes, 35 = weak, 90 = none				
14. folpust	133 = yes, 3 = none				
17. pntfol	62 = curved, 74 = straight				
33. thckrad	1 = yes, 105 = none				
Coiling direction	30 = right, 102 = left				
Microspheric	3 = yes, 127 = no				
(c) <i>Ammonia tepida</i>					
12 intact, 41 not completely measured specimens					
	<i>n</i>	Minimum	Maximum	Mean	1 σ
1. gsd	40	96.61	324.37	172.57	71.83
2. gsd/h	29	1.596	2.211	1.845	0.149
3. hs/hu	29	0.773	1.758	1.232	0.251
7. du	49	13.35	78.91	32.41	18.60
8. rfl/w	46	0.52	1.02	0.77	0.12
9. maxbos	18	4.91	24.04	11.28	5.43
21. prol (micro)	4	9	13	11	1.6
21. prol (mega)	48	20	63	34	11.0
22. chwh1	50	5	9	6.5	0.8
25. ch	46	7	19	12.1	3.2
26. Lc/wc	42	0.77	2.19	1.39	0.33
27. perout	49	0	91.5	38.2	32.3
28. spfis	23	11.7	71.5	28.5	17.2
29. rad $\hat{}$	45	61.7	128.5	88.8	14.9
36. mnpor	48	0.34	0.73	0.54	0.10
11. nobos	31 = none, 17 = 1, 1 = 2 umbonal bosses				
13. thckfol	5 = yes, 6 = weak, 38 = none				
14. folpust	49 = yes, 1 = none				
17. pntfol	46 = curved, 4 = straight				
33. thckrad	1 = yes, 49 = none				
Coiling direction	15 = right, 37 = left				
Microspheric	4 = yes, 48 = no				

Table B6. Continued.

(d) <i>Ammonia bellaria</i> n. sp.					
17 intact, 37 not completely measured specimens					
	<i>n</i>	Minimum	Maximum	Mean	1σ
1. gsd	49	94.59	190.26	130.76	22.41
2. gsd/h	45	1.473	2.184	1.800	0.137
3. hs/hu	45	0.707	1.948	1.271	0.292
7. du	52	13.93	36.96	23.16	5.14
8. rfl/w	50	0.51	0.99	0.81	0.12
9. maxbos	23	3.26	15.01	8.0	2.67
21. prol (micro)	6	9	15	11	2.1
21. prol (mega)	45	20	50	29	5.5
22. chwh1	51	5	8	6.4	0.6
25. ch	42	5	16	10.7	2.9
26. Lc/wc	53	0.73	2.64	1.48	0.42
27. perout	48	0	100.0	41.6	37.3
28. spfis	34	12.1	60.9	22.2	9.6
29. rad [^]	53	65.6	106.3	86.5	9.2
36. mnpor	53	0.26	0.75	0.51	0.09
11. nobos	29 = none, 20 = 1, 3 = 2 umbonal bosses				
13. thckfol	6 = weak, 46 = none				
14. folpust	41 = yes, 11 = none				
17. pntfol	48 = curved, 4 = straight				
33. thckrad	3 = yes, 50 = none				
Coiling direction	30 = right, 23 = left				
Microspheric	6 = yes, 45 = no				
(e) <i>Ammonia beccarii</i> (dead specimens)					
1 intact, 1 not completely measured specimen					
		Minimum	Maximum	Mean	
1. gsd			343.85		
2. gsd/h	1.937	2.260		2.098	
3. hs/hu	0.771	0.886		0.829	
7. du	71.93	72.79		72.36	
8. rfl/w	0.94	1.01		0.98	
9. maxbos	23.21	33.97		28.59	
21. prol	51	67		59	
22. chwh1	7	8		8	
25. ch	8	12		10	
26. Lc/wc	0.75	0.82		0.79	
27. perout	65.8	69.1		67.5	
28. spfis	41.2	45.9		43.5	
29. rad [^]	91.5	100.7		96.1	
36. mnpor	1.2	1.7		1.4	
11. nobos	1 = 1, 1 = 2 umbonal bosses				
13. thckfol	2 = yes				
14. folpust	2 = yes				
17. pntfol	2 = curved				
18. radbd	2 = yes				
33. thckrad	2 = yes				
Coiling direction	2 = left				
Microspheric	2 = no				

Table B7. Range of numerical values for selected biometric parameters of *Ammonia* species considered in this study after Hayward et al. (2004), supplemented by Hayward et al. (2019); values partially amended following Hayward et al. (2021) (see Table B2 for abbreviations). The values of gsd, maxbos, and prol are given in millimetres (mm), with mnpore given in micrometres (µm). The values of perout are given in percent, and rad[°] is given in degrees by the authors. *aberdov.*: *aberdoveyensis*, *parkinson.*: *parkinsoniana*.

	<i>A. veneta</i>	<i>A. aberdov.</i>	<i>A. parkins.</i>	<i>A. beccarii</i>	<i>A. tepida</i>
1. gsd	0.22–0.43	0.29–0.51	0.45–0.70	0.58–1.70	0.20–0.30
2. gsd/h	1.7–2.3	1.9–2.3	2.0–2.5	2.1–3.9	2.0–3.0
3. hs/hu	0.8–2.4	0.6–1.4	0.9–2.0	0.6–1.4	1.5–2.0
8. rf/w	0.5–0.7	0.4–0.8	0.4–0.9	0.85–1.0	0.2–0.95
9. maxbos	0–0.03	0–0.05	0.1–0.11	0.07–0.25	–
21. prol	0.05–0.08	0.03–0.06	0.07	0.03–0.11	0.03–0.05
22. chwh1	6.5–8	6.5–10	8–13	7–16	5.5–6.5
26. lc/wc	1.2–2.5	0.9–2.4	1.0–1.2	0.7–1.0	1.4–1.8
27. perout	0–70	0–70	50–80	50–100	0
29. rad [°]	70–90	65–80	90	90–100	80–90
36. mnpor	1.0–2.5	0.5–1.5	0.5–1.5	1.2–2.1	0.3–0.9

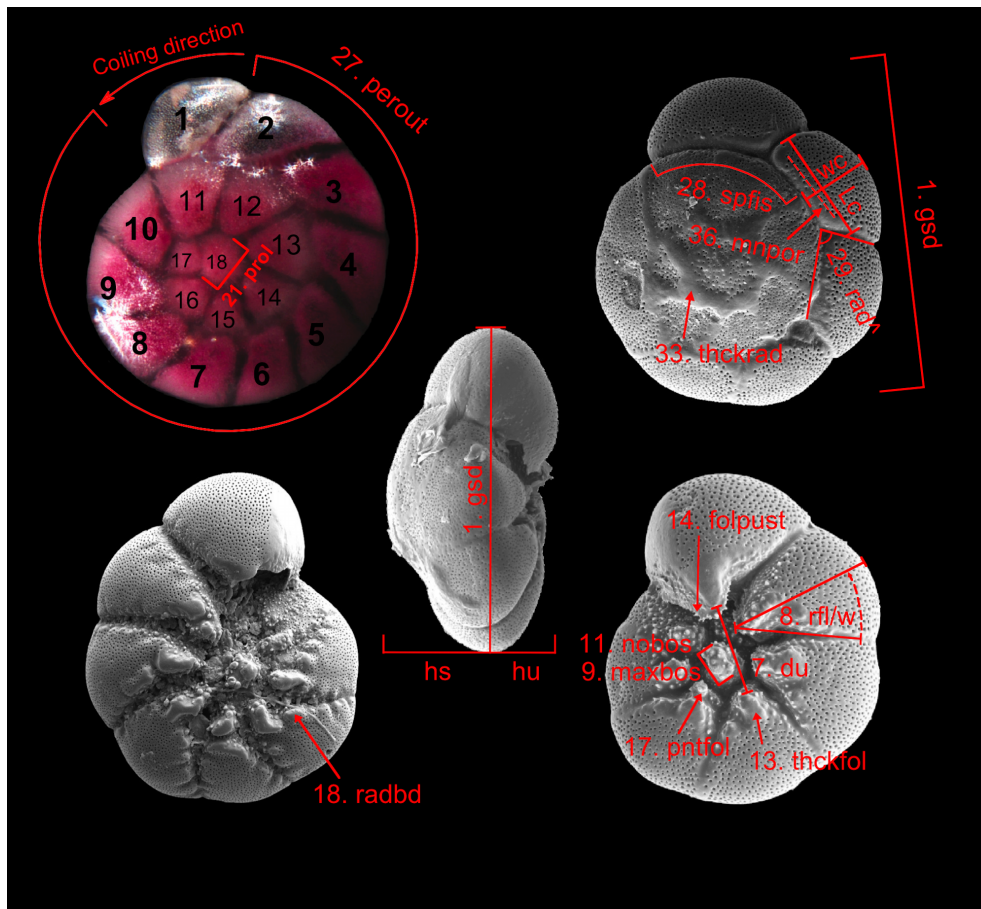


Figure B1. Parameters measured and assessed from microscopic images of *Ammonia* specimens. The abbreviations are explained in Table B2. Not to scale.

Data availability. The holotype, paratype, all imaged specimens, and a portion of the untouched residues are deposited in the Micropaleontological Collections held at the Natural History Museum, Basel. The data discussed in this paper are available in Tables 1–7.

Supplement. The biometric measurements are available as an online Supplement to this paper (file: Supplement_Ammonia_biometric_data_species_rev.xls). The supplement related to this article is available online at: <https://doi.org/10.5194/jm-40-195-2021-supplement>.

Author contributions. VB performed the sampling, sample preparation, light microscopic, and SEM imaging. The species were determined by all authors in consensus. Morphometric analyses were performed by JS and SaS, with help from a work student and an intern. The statistics were done by SaS. The taxonomic descriptions were performed by SiS. JS prepared the paper with contributions from all coauthors.

Competing interests. The contact author has declared that neither they nor their coauthors have any competing interests.

Disclaimer. Publisher's note: Copernicus Publications remains neutral with regard to jurisdictional claims in published maps and institutional affiliations.

Acknowledgements. Simone Negri helped the second author during fieldwork, and Davide Quadrelli provided the boat at Bellaria. Carina Schönhofen and Zeynep Akgüc (Kiel, Germany) measured parts of the light microscopic and SEM images with great accuracy. Thorsten Lemke (Lemke Software GmbH, Peine, Germany) sponsored a GraphicConverter license, for which we thank him. Bruce Hayward (Auckland, New Zealand), Martin Langer (Bonn, Germany), Anna Weinmann (Vienna, Austria), Magali Schweizer (Angers, France), Rossana Serandrei-Barbero (Venice, Italy), Orit Hyams (Jerusalem, Israel), and Alberto Albani (Sydney, Australia) provided rare literature, advice on Mediterranean foraminifera, and information on *Ammonia* genotype denominations. Stefan Meng, Peter Michalik (Greifswald University, Germany), Karl Schilling, and Markus Lambertz (Bonn University, Germany) screened the museum and institute collections for yet unlocated material from Max Schultze. Horst Kuhn and Alfons Renz (Tübingen, Germany) provided information on the capabilities of historical microscopes. Michael Knappertsbusch hosts the specimens at the Natural History Museum in Basel, Switzerland, which is gratefully acknowledged. Financial contributions to Silvia Spezzaferrri and Valentina Beccari were provided by the Swiss National Science Foundation under project ref. 200021_175587.

Financial support. The article processing charges for this open-access publication were covered by the GEOMAR Helmholtz Centre for Ocean Research Kiel.

Review statement. This paper was edited by Laia Alegret and reviewed by two anonymous referees.

References

- Alve, E.: Benthic foraminifera in sediment cores reflecting heavy metal pollution in Soerfjord, Western Norway, *J. Foramin. Res.*, 21, 1–19, <https://doi.org/10.2113/gsjfr.21.1.1>, 1991.
- Alve, E., Korsun, S., Schönfeld, J., Dijkstra, N., Golikova, E., Hess, S., Husum, K., and Panieri, G.: ForAM-BI: a sensitivity index based on benthic foraminiferal faunas from North-East Atlantic and Arctic fjords, continental shelves and slopes, *Mar. Micropaleontol.*, 122, 1–12, <https://doi.org/10.1016/j.marmicro.2015.11.001>, 2016.
- Alve, E., Hess, S., Bouchet, V. M. P., Dolven, J. K., and Rygg, B.: Intercalibration of benthic foraminiferal and macrofaunal biotic indices: an example from the Norwegian Skagerrak coast (NE North Sea), *Ecol. Indic.*, 96, 107–115, <https://doi.org/10.1016/j.ecolind.2018.08.037>, 2019.
- Artegiani, A., Bregant, D., Paschini, E., Pinardi, N., Raicich, F., and Russo, A.: The Adriatic Sea general circulation, Part II: baroclinic circulation structure, *J. Phys. Oceanogr.*, 27, 1515–1532, [https://doi.org/10.1175/1520-0485\(1997\)027](https://doi.org/10.1175/1520-0485(1997)027), 1997.
- Barbero, R. S., Albani, A. D., and Donnici, S.: *Atlante dei foraminiferi della laguna di Venezia*, Istituto Veneto di Scienze, Lettere ed Arti, Venezia (Italia), 120 pp., ISBN-10: 8895996046, 2008.
- Barras, C., Jorissen, F. J., Labrune, C., Andral, B., and Boissery, P.: Live benthic foraminiferal faunas from the French Mediterranean Coast: towards a new biotic index of environmental quality, *Ecol. Indic.*, 36, 719–743, <https://doi.org/10.1016/j.ecolind.2013.09.028>, 2014.
- Bé, A. W. H.: Ecology of recent planktonic foraminifera: Part I – Areal distribution in the western North Atlantic, *Micropaleontology*, 5, 77–100, <https://doi.org/10.2307/1484157>, 1959.
- Benton, M. J. and Pearson, P. N.: Speciation in the fossil record, *Trend. Ecol. Evol.*, 16, 405–411, [https://doi.org/10.1016/S0169-5347\(01\)02149-8](https://doi.org/10.1016/S0169-5347(01)02149-8), 2001.
- Bird, C., Schweizer, M., Roberts, A., Austin, W. E. N., Knudsen, K. L., Evans, K. M., Filipsson, H. L., Sayer, M. D. J., Geslin, E., and Darling, K. F.: The genetic diversity, morphology, biogeography, and taxonomic designations of *Ammonia* (Foraminifera) in the Northeast Atlantic, *Mar. Micropaleontol.*, 155, 101726, <https://doi.org/10.1016/j.marmicro.2019.02.001>, 2020.
- Boltovskoy, E., Giussani, G., Watanabe, S., and Wright, R.: *Atlas of benthic shelf Foraminifera of the Southwest Atlantic*, Dr. W. Jung bv Publishers, The Hague, 146 pp., <https://doi.org/10.1007/978-94-009-9188-0>, 1980.
- Bouchet, V. M. P., Alve, E., Rygg, B., and Telford, R. J.: Benthic foraminifera provide a promising tool for ecological quality assessment of marine waters, *Ecol. Indic.*, 23, 66–75, <https://doi.org/10.1016/j.ecolind.2012.03.011>, 2012.
- Bouchet, V. M. P., Frontalini, F., Francescangeli, F., Sauriau, P.-G., Geslin, E., Martins, M. V. A., Almogi-Labin, A., Avnaim-Katav, S., Di Bella, L., Cearreta, A., Coccioni, R., Costelloe, A., Dimiza, M. D., Ferraro, L., Haynert, K., Martínez-Coloin, M., Melis, R., Schweizer, M., Triantaphyllou, M. V., Tsujimoto, A., Wilson, B., and Armynot du Cha?telet, E.: Indicative value of benthic

- foraminifera for biomonitoring: assignment to ecological groups of sensitivity to total organic carbon of species from European intertidal areas and transitional waters, *Mar. Pollut. Bull.*, 164, 112071, <https://doi.org/10.1016/j.marpolbul.2021.112071>, 2021.
- Bradshaw, J. D.: Laboratory experiments on the ecology of foraminifera, *Contributions from Cushman Foundation for Foraminiferal Research*, 12, 87–106, <https://doi.org/10.4236/ojg.2015.54020>, 1961.
- Bradshaw, J. D.: Environmental parameters and marsh foraminifera, *Limnol. Oceanogr.*, 13, 26–38, <https://doi.org/10.4319/lo.1968.13.1.0026>, 1968.
- Brünnich, M. T.: *Zoologiae fundamenta, Praelectionibus Academicis Accommodata, Grunde i Dyeloeren, Hafniae et Lipsiae*, Copenhagen, 253 pp., <https://doi.org/10.5962/bhl.title.42672>, 1771.
- Chayes, F.: A simple point counter for thin-section analysis, *Am. Mineral.*, 34, 1–11, <https://pubs.geoscienceworld.org/msa/ammin/article/34/1-2/1541208/1949>, 1949.
- Cifelli, R.: The Morphology and structure of *Ammonia beccarii* (Linne), *Contributions from the Cushman Foundation for Foraminiferal Research*, 13, 119–127, 1962.
- Cimerman, F. and Langer, M. R.: Mediterranean foraminifera, *Slovenska Akademija Znanosti in Umetnosti. Academia Scientiarum et Artium Slovenica, Classis 4, Historia Naturalis*, 30, 1–118, ISBN: 8671310531 9788671310536, 1991.
- Cushman, J. A.: Recent foraminifera from Puerto Rico, *Publications of the Carnegie Institution of Washington*, 342, 73–84, 1926.
- Cushman, J. A.: On *Rotalia beccarii* (Linne), *Contributions from the Cushman Laboratory for Foraminiferal Research*, 4, 103–107, 1928.
- d'Orbigny, A.: *Tableau Methodique de la Classe des Cephalopodes*, *Ann. Sci. Nat.*, 7, 96–314, 245–314, 1826.
- d'Orbigny, A.: Foraminifères, in: *Histoire physique, politique et naturelle de L'île de Cuba*, edited by: De la Sagra, R. M. and Bertrand, A., Paris, 1–224, <https://doi.org/10.5962/bhl.title.51128>, 1839.
- Darling, K. F., Schweizer, M., Knudsen, K. L., Evans, K. M., Bird, C., Roberts, A., Filipsson, H. L., Kim, J.-H., Gudmundsson, G., Wade, C. M., Sayer, M. D. J., and Austin, W. E. N.: The genetic diversity, phylogeography and morphology of *Elphidiidae* (Foraminifera) in the Northeast Atlantic, *Mar. Micropaleontol.*, 129, 1–23, <https://doi.org/10.1016/j.marmicro.2016.09.001>, 2016.
- Debenay, J.-P., Beneteau, E., Zhang, J., Stoff, V., Geslin, E., Redois, F., and Fernandez-Gonzalez, M.: *Ammonia beccarii* and *Ammonia tepida* (Foraminifera): morphofunctional arguments for their distinction, *Mar. Micropaleontol.*, 34, 235–244, [https://doi.org/10.1016/S0377-8398\(98\)00010-3](https://doi.org/10.1016/S0377-8398(98)00010-3), 1998.
- de Chanvalon, T. A., Metzger, E., Mouret, A., Cesbron, F., Knor, J., Rozuel, E., Launeau, P., Nardelli, M. P., Jorissen, F. J., and Geslin, E.: Two-dimensional distribution of living benthic foraminifera in anoxic sediment layers of an estuarine mudflat (Loire Estuary, France), *Biogeosciences*, 12, 6219–6234, <https://doi.org/10.5194/bg-12-6219-2015>, 2015.
- Delage, Y. and Heirouard, E.: *Traite de Zoologie Concrète. Volume 1. La Cellule et les Protozoaires, Schleicher et Frères, Paris*, 584 pp., <https://doi.org/10.5962/bhl.title.11672>, 1896.
- Deldicq, N., Alve, E., Schweizer, M., Asteman, I.P., Hess, S., Darling, K., and Bouchet, V. M. P.: History of the introduction of a species resembling the benthic foraminifera *Nonionella stella* in the Oslofjord (Norway): Morphological, molecular and paleoecological evidences, *Aquatic Invasions*, 14, 182–205, <https://doi.org/10.3391/ai.2019.14.2.03>, 2019.
- de Nooijer, L.: Shallow-water benthic foraminifera as proxy for natural versus human-induced environmental change, *Geologica Ultraiectina*, 272, 1–152, ISBN 90-5744-136-5 2007.
- De Queiroz, K.: Species concepts and species delimitation, *System. Biol.*, 56, 879–886, <https://doi.org/10.1080/10635150701701083>, 2007.
- Diz, P. and Francés, G.: Distribution of live benthic foraminifera in the Riia de Vigo (NW Spain), *Mar. Micropaleontol.*, 66, 165–191, <https://doi.org/10.1016/j.marmicro.2007.09.001>, 2008.
- Donnici, S. and Barbero, R. S.: The benthic foraminiferal communities of the northern Adriatic continental shelf, *Mar. Micropaleontol.*, 44, 93–123, [https://doi.org/10.1016/S0377-8398\(01\)00043-3](https://doi.org/10.1016/S0377-8398(01)00043-3), 2002.
- Donnici, S., Serandrei Barbero, R., and Taroni, G.: Living Benthic Foraminifera in the Lagoon of Venice (Italy): Population Dynamics and its Significance, *Micropaleontology*, 43, 440–454, <https://doi.org/10.2307/1485933>, 1997.
- Drooger, C. W.: Radial Foraminifera, morphometrics and evolution, *Verhandelingen der Koninklijke Akademie van Wetenschappen, Afdeling Natuurkunde, Eerste Sectie*, 41, 1–242, 1993.
- Dupuy, C., Rossignol, L., Geslin, E., and Pascal, P. Y.: Predation of mudflat meio-macrofaunal metazoans by a calcareous foraminifer, *Ammonia tepida* (Cushman 1926), *J. Foramin. Res.*, 40, 305–312, <https://doi.org/10.2113/gsjfr.40.4.305>, 2010.
- Ehrenberg, C. G.: Über die Bildung der Kreidelfelsen und des Kreidemergels durch unsichtbare Organismen. *Königlichen Akademie der Wissenschaften zu Berlin, Physikalische Abhandlungen*, 1838, 59–147, 1839.
- Ehrenberg, C. G.: Eine weitere Erläuterung des Organismus mehrerer in Berlin lebend beobachteter Polythalamien der Nordsee, *Bericht über die zur Bekanntmachung geeigneten Verhandlungen der Königlichen Preussischen Akademie der Wissenschaften zu Berlin*, 1840, 18–23, 1840.
- Ehrenberg, C. G.: Über noch jetzt zahlreich lebende Thierarten der Kreidebildung und den Organismus der Polythalamien, *Königliche Akademie der Wissenschaften Berlin, Physikalische Abhandlungen*, 1839, 81–174, 1841.
- Ellis, B. F. and Messina, A.: *Catalogue of Foraminifera*, *Micropaleontology Press, New York*, available at: <http://www.micropress.org> (last access: 5 December 2020), 1940.
- Francescangeli, F., Milker, Y., Bunzel, D., Thomas, H., Norbisch, M., Schönfeld, J., and Schmiedl, G.: Recent benthic foraminiferal distribution in the Elbe Estuary (North Sea, Germany): A response to environmental stressors, *Estuarine, Coast. Shelf Sci.*, 251, 107198, <https://doi.org/10.1016/j.ecss.2021.107198>, 2021.
- Haake, F.-W.: Living benthic foraminifera in the Adriatic Sea: Influence of water depth and sediment, *J. Foramin. Res.*, 7, 62–75, <https://doi.org/10.2113/gsjfr.7.1.62>, 1977.
- Hammer Ø., Harper, D. A. T., and Ryan, P. D.: PAST: Paleontological statistics software package for education and data analysis, *Palaeontol. Electron.*, 4, p. 9, 2001.

- Hayek, L.-A. C., Buzas, M. A., Buzas-Stephens, P., and Buzas, J. S.: On replicates for comparing species densities in space and time, *J. Foramin. Res.*, 51, 92–97, <https://doi.org/10.2113/gsjfr.51.2.92>, 2021.
- Haynert, K., Gluderer, F., Pollierer, M. M., Scheu, S., and Wehrmann, A.: Food spectrum and habitat-specific diets of benthic foraminifera from the Wadden Sea – a fatty acid biomarker approach, *Front. Mar. Sci.*, 7, 510288, <https://doi.org/10.3389/fmars.2020.510288>, 2020.
- Haynes, J. R.: Cardigan Bay recent Foraminifera (Cruises of the R.V. Antur, 1962–1964), British Museum (Natural History), Zoology. Supplement, 4, 1–245, 1973.
- Hayward, B. W., Holzmann, M., Grenfell, H. R., Pawlowski, J., and Triggs, C.M.: Morphological distinction of molecular types in *Ammonia* – towards a taxonomic revision of the world's most commonly misidentified foraminifera, *Mar. Micropaleontol.*, 50, 237–271, [https://doi.org/10.1016/S0377-8398\(03\)00074-4](https://doi.org/10.1016/S0377-8398(03)00074-4), 2004.
- Hayward, B. W., Holzmann, M., and Tsuchiya, M.: Combined molecular and morphological taxonomy of the beccarii/T3 group of the foraminiferal genus *Ammonia*, *J. Foramin. Res.*, 49, 367–389, <https://doi.org/10.2113/gsjfr.49.4.367>, 2019.
- Hayward, B. W., Holzmann, M., Pawlowski, J., Parker, J. H., Kaushik, T., Toyofuku, M. S., and Tsuchiya, M.: Molecular and morphological taxonomy of living *Ammonia* and related taxa (Foraminifera) and their biogeography, *Micropaleontology*, 67, 109–313, available at: <https://www.micropress.org/microaccess/micropaleontology/issue-368/article-2228>, last access: 21 November 2021.
- Heron-Allen E. and Earland A.: On some Foraminifera from the North Sea dredged by the Fisheries Cruiser “Huxley” (International North Sea Investigations – England), *Journal of the Quekett Microscopical Club*, 12, 121–138, <https://doi.org/10.1111/j.1365-2818.1912.tb04934.x>, 1913.
- Hohenegger, J.: Larger foraminifera-microscopical greenhouses indicating shallow-water tropical and subtropical environments in the present and past, Kagoshima University Research Center for the Pacific Islands, Occasional Papers, 32, 19–45, 1999.
- Holzmann, M.: Species concept in Foraminifera: *Ammonia* as a case study, *Micropaleontology*, 46, 21–37, 2000.
- Holzmann, M. and Pawlowski, J.: Molecular, morphological, and ecological evidence for species recognition in *Ammonia* (Foraminifera), *J. Foramin. Res.*, 27, 311–318, [https://doi.org/10.1016/S0377-8398\(03\)00074-4](https://doi.org/10.1016/S0377-8398(03)00074-4), 1997.
- Holzmann, M., Piller, W., Fenner, R., Martini, R., Serandrei-Barbero, R., and Pawlowski, J.: Morphologic versus molecular variability in *Ammonia* spp. (Foraminifera, Protozoa) from the Lagoon of Venice, Italy, *Rev. Micropaleontol.*, 41, 59–69, [https://doi.org/10.1016/S0035-1598\(98\)90098-8](https://doi.org/10.1016/S0035-1598(98)90098-8), 1998.
- Hottinger, L.: Comparative anatomy of elementary shell structures in selected larger foraminifera, in: Foraminifera, Vol. 3, edited by: Hedley, R. H. and Adams, C. G., Academic Press, London, 203–266, 1978.
- Hottinger, L.: Illustrated glossary of terms used in foraminiferal research, Carnets de Géologie/Notebooks on Geology Memoir, 2006/02, 1–126, <https://doi.org/10.4267/2042/5832>, 2006.
- Jorissen, F. J.: Benthic foraminifera from the Adriatic Sea; principles of phenotypic variation, *Utrecht Micropaleontological Bulletin*, 37, 7–139, ISSN 0083-4963, 1988.
- Jorissen, F. J., Nardelli, M. P., Almogi-Labin, A., Barras, C., Bergamin, L., Bicchi, E., El Kateb, A., Ferraro, L., McGann, M., Morigi, C., Romano, E., Sabbatini, A., Schweizer, M., and Spezzaferri, S.: Developing Foram-AMBI for biomonitoring in the Mediterranean: species assignments to ecological categories, *Mar. Micropaleontol.*, 140, 33–45, <https://doi.org/10.1016/j.marmicro.2017.12.006>, 2018.
- Keul, N., Langer, G., de Nooijer, L. J., and Bijma, J.: Effect of ocean acidification on the benthic foraminifera *Ammonia* sp. is caused by a decrease in carbonate ion concentration, *Biogeosciences*, 10, 6185–6198, <https://doi.org/10.5194/bg-10-6185-2013>, 2013.
- Koho, K. A., LeKieffre, C., Nomaki, H., Salonen, I., Geslin, E., Mabilieu, G., Sjøgaard Jensen, L. H., and Reichart, G.-J.: Changes in ultrastructural features of the foraminifera *Ammonia* spp. in response to anoxic conditions: Field and laboratory observations, *Mar. Micropaleontol.*, 138, 72–82, <https://doi.org/10.1016/j.marmicro.2017.10.011>, 2018.
- Labaj, P., Topa, P., Tyszká, J., and Alda, W.: 2D and 3D numerical models of the growth of foraminiferal shells, *Lect. Notes Comput. Sci.*, 2657, 669–678, https://doi.org/10.1007/3-540-44860-8_69, 2003.
- Langer, M., Hottinger, L., and Huber, B.: Functional morphology in low-diverse benthic foraminiferal assemblages from tidal flats of the North Sea, *Senck. Marit.*, 20, 81–99, ISSN 0080-889X, 1989.
- Lehmann, G.: Vorkommen, Populationsentwicklung, Ursache flächenhafter Besiedlung und Fortpflanzungsbiologie von Foraminiferen in Salzwiesen und Flachwasser der Nord- und Ostseeküste Schleswig-Holsteins, Dissertation, Christian-Albrechts-Universität zu Kiel, Germany, 218 pp., available at: http://macau.uni-kiel.de/receive/dissertation_diss_413 (last access: 21 November 2021), 2000.
- LeKieffre, C., Spangenberg, J. E., Mabilieu, G., Escrig, S., Meibom, A., and Geslin, E.: Surviving anoxia in marine sediments: The metabolic response of ubiquitous benthic foraminifera (*Ammonia tepida*), *PLoS ONE*, 12, e0177604, <https://doi.org/10.1371/journal.pone.0177604>, 2017.
- Less, G. and Kovács, L. Oi.: Typological versus morphometric separation of orthophragminid species in single samples – a case study from Horsarrieu (upper Ypresian, SW Aquitaine, France), Seiparation typologique et morphométrique des espèces d'Orthophragmines dans des échantillons isolés – application à un échantillon provenant de Horsarrieu (Ypresien supérieur, Sud-Ouest de l'Aquitaine, France), *Revue de Micropaleontologie*, 52, 267–288, <https://doi.org/10.1016/j.revmic.2008.10.001>, 2009.
- Li, M., Lei, Y., Li, T., and Dong, S.: Response of intertidal foraminiferal assemblages to salinity changes in a laboratory culture experiment, *J. Foramin. Res.*, 50, 319–329, <https://doi.org/10.2113/gsjfr.50.4.319>, 2020.
- Linné, C.: Systemae naturae, edition 10, tomus 1, Stockholm, Sweden, 710 pp., available at: <https://www.biodiversitylibrary.org/page/726886> (last access: 21 November 2021), 1758.
- Lister, J. J.: Contributions to the life-history of the Foraminifera, *Philos. Trans. Roy. Soc.*, B186, 401–453, <https://doi.org/10.1098/rstb.1895.0008>, 1895.
- Montanari, R. and Marasmi, C.: New tools for coastal management in Emilia-Romagna, Regione Emilia-Romagna, Assessorato alla Sicurezza Territoriale Difesa del Suolo e della Costa Protezione Civile, Bologna, Italy, 72 pp., 2012.

- Moodley, L. and Hess, C.: Tolerance of infaunal benthic foraminifera for low and high oxygen concentrations, *Biol. Bull.*, 183, 94–98, <https://doi.org/10.2307/1542410> 1992.
- Morigi, C., Jorissen, F. J., Fraticelli, S., Horton, B. P., Principi, M., Sabbatini, A., Capotondi, L., Curzi, P. V., and Negri, A.: Benthic foraminiferal evidence for the formation of the Holocene mud-belt and bathymetrical evolution in the central Adriatic Sea, *Mar. Micropaleontol.*, 57, 25–49, <https://doi.org/10.1016/j.marmicro.2005.06.001>, 2005.
- Mouanga, G. H.: Impact and range extension of invasive foraminifera in the NW Mediterranean Sea: Implications for diversity and ecosystem functioning, Dissertation, Universität Bonn, Bonn, 230 pp., available at: <https://bonndoc.ulb.uni-bonn.de/xmlui/handle/20.500.11811/7491> (last access: 21 November 2021), 2017.
- Murray, J. W.: Ecology and Palaeoecology of Benthic Foraminifera, Longman Scientific & Technical, Essex, United Kingdom, 397 pp., <https://doi.org/10.4324/9781315846101>, 1991.
- Murray, J. W.: Unravelling the life cycle of “*Polystomella crispa*”: the roles of Lister, Jepps and Myers, *J. Micropalaeontol.*, 31, 121–129, <https://doi.org/10.1144/0262-821X11-034>, 2012.
- Murray, J. W.: Some trends in sampling modern living (stained) benthic foraminifera in fjord, shelf and deep sea: Atlantic Ocean and adjacent seas, *J. Micropalaeontol.*, 34, 101–104, <https://doi.org/10.1144/jmpaleo2014-004>, 2015.
- Murray, J. W. and Alve, E.: Major aspects of foraminiferal variability (standing crop and biomass) on a monthly scale in an intertidal zone, *J. Foramin. Res.*, 30, 177–191, <https://doi.org/10.2113/0300177>, 2000.
- Myers, E. H.: Life activities of foraminifera in relation to marine ecology, *Am. Philos. Soc. Proceed.*, 86, 439–458, 1943.
- Natland, M. L.: New species of Foraminifera from off the west coast of North America and from the later Tertiary of the Los Angeles basin, *Bulletin of the Scripps Institution of Oceanography of the University of California, Tech. Ser.*, 4, 137–163, 1938.
- Nixon, K. C. and Wheeler, Q. D.: An amplification of the phylogenetic species concept, *Cladistics*, 6, 211–223, <https://doi.org/10.1111/j.1096-0031.1990.tb00541.x>, 1990.
- Otto, G. H.: A modified logarithmic probability graph for the interpretation of mechanical analyses of sediments, *J. Sediment. Res.*, 9, 62–76, <https://doi.org/10.1306/D4269044-2B26-11D7-8648000102C1865D>, 1939.
- Parent, B., Hyams-Kaphzan, O., Barras, C., Lubinevsky, H., and Jorissen, F.: Testing foraminiferal environmental quality indices along a well-defined organic matter gradient in the Eastern Mediterranean, *Ecol. Indic.*, 125, 107498, <https://doi.org/10.1016/j.ecolind.2021.107498>, 2021.
- Pascal, P.-Y., Dupuy, C., Richard, P., and Niquil, N.: Bacterivory in the common foraminifer *Ammonia tepida*: isotope tracer experiment and the controlling factors, *J. Exp. Mar. Biol. Ecol.*, 359, 55–61, <https://doi.org/10.1016/j.jembe.2008.02.018>, 2008.
- Pawłowski, J., Holzmann, M., and Tyszk, J.: New supraordinal classification of foraminifera: molecules meet morphology, *Mar. Micropaleontol.*, 100, 1–10, <https://doi.org/10.1016/j.marmicro.2013.04.002>, 2013.
- Plancus, J.: *Jani Planci Ariminensis de conchis minus notis*, tomus 56, Venetis, available at: <https://www.biodiversitylibrary.org/page/15178957> (last access: 21 November 2021), 1739.
- Poag, C. W.: Paired foraminiferal ecophenotypes in Gulf Coast estuaries: Ecological and paleoecological implications, *Transactions of the Gulf Coast Assoc. Geol. Soc.*, 28, 395–421, 1978.
- Polovodova, I. and Schönfeld, J.: Foraminiferal test abnormalities in the western Baltic Sea, *J. Foramin. Res.*, 38, 318–336, <https://doi.org/10.2113/gsjfr.38.4.318>, 2008.
- Preti, M.: Ripascimento di spiagge con sabbie sottomarine in Emilia-Romagna, *Studi Costieri*, 5, 107–134, available at: <http://oceanrep.geomar.de/id/eprint/53247> (last access: 21 November 2021), 2000.
- Prioli, I.: Difesa della Costa, l’Emilia-Romagna anticipa il Recovery: 22 milioni di euro per il ripascimento di 15 km di spiagge, available at: <https://www.regione.emilia-romagna.it/notizie/2021/>, last access: 8 Juni 2021.
- Raw, F.: The development of *Leptoplastus salteri* and other trilobites, *Q. J. Geol. Soc. Lond.*, 81, 223–324, <https://doi.org/10.1144/GSL.JGS.1925.081.01-04.12>, 1925.
- Richirt, J., Schweizer, M., Bouchet, V. M. P., Mouret, A., Quinchard, S., and Jorissen, F. J.: Morphological distinction of three *Ammonia* phylotypes occurring along European coasts, *J. Foramin. Res.*, 49, 76–93, <https://doi.org/10.2113/gsjfr.49.1.76>, 2019.
- Richirt, J., Schweizer, M., Mouret, A., Quinchard, S., Saad, S. A., Bouchet, V. M. P., Wade, C. M., and Jorissen, F. J.: Biogeographic distribution of three phylotypes (T1, T2 and T6) of *Ammonia* (foraminifera, Rhizaria) around Great Britain: new insights from combined molecular and morphological recognition, *J. Micropalaeontol.*, 40, 61–74, <https://doi.org/10.5194/jm-40-61-2021>, 2021.
- Richter, G.: Beobachtungen zur Ökologie einiger Foraminiferen des Jade-Gebietes, *Natur und Museum*, 91, 163–170, 1961.
- Roberts, A., Austin, W., Evans, K., Bird, C., Schweizer, M., and Darling, K.: A new integrated approach to taxonomy: the fusion of molecular and morphological systematics with type material in benthic foraminifera, *PLoS One*, 11, e0158754, <https://doi.org/10.1371/journal.pone.0158754>, 2016.
- Rouvillois, A.: Un foraminifère méconnu du plateau continental du golfe de Gascogne: *Pseudoeponides falsebecarii* n. sp., *Cahiers de Micropalaeontologie*, 3, 3–7, 1974.
- Saidova, Kh. M.: O sovremennom sostoyanii sistemi nadvidovykh taksonov Kaynozoyskikh bentosnykh foraminifer, Institut Okeanologii P.P. Shirshova, Akademiya Nauk SSR, Moscow, 73 pp., 1981.
- Schönfeld, J. and Voigt, T.: Sediment geometry, facies analysis and palaeobathymetry of the Schrammstein Formation (upper Turonian–lower Coniacian) in southern Saxony, Germany, *Z. Dtsch. Ges. Geowiss.*, 171, 199–209, <https://doi.org/10.1127/zdgg/2020/0220>, 2020.
- Schönfeld, J., Alve, E., Geslin, E., Jorissen, F., Korsun, S., and Spezzaferri, S.: The FOBIMO (FOraminiferal Bio-MONitoring) initiative – towards a standardised protocol for benthic foraminiferal monitoring studies, *Mar. Micropaleontol.*, 94–95, 1–13, <https://doi.org/10.1016/j.marmicro.2012.06.001>, 2012.
- Schultze, M. J. S.: über den Organismus der Polythalamien (Foraminiferen), nebst Bemerkungen über die Rhizopoden im allgemeinen, Ingelmann, Leipzig, 68 pp., available at: https://books.google.pt/books?id=o7rk00_xueQC (last access: 21 November 2021), 1854.

- Schweizer, M., Polovodova, I., Nikulina, A., and Schönfeld, J.: Molecular identification of *Ammonia* and *Elphidium* species (Foraminifera, Rotaliida) from the Kiel Fjord (SW Baltic Sea) with rDNA sequences, *Helgoland Mar. Res.*, 65, 1–10, <https://doi.org/10.1007/s10152-010-0194-3>, 2011.
- Sen, A. and Bhadury, P.: Exploring the seasonal dynamics within the benthic foraminiferal biocoenosis in a tropical monsoon-influenced coastal lagoon, *Aquat. Biol.*, 25, 121–138, <https://doi.org/10.3354/ab00658>, 2016.
- Serandrei-Barbero, R., Albani, A. D., and Donnici, S.: *Atlante dei Foraminiferi della Laguna di Venezia*, Istituto Veneto di Scienze, Lettere ed Arti, Venezia, 164 pp., 2008.
- Seuront, L. and Bouchet, V. M. P.: The devil lies in details: new insights into the behavioural ecology of intertidal foraminifera, *J. Foramin. Res.*, 45, 390–401, <https://doi.org/10.2113/gsjfr.45.4.390>, 2015.
- Simmons, M. and Bidgood, M.: Thinking about species, *Newsletter of Micropalaeontology*, 103, 37–41, 2021.
- Simonini, R., Ansaloni, I., Bonvicini Pagliai, A. M., Cavallini, F., Iotti, M., Mauri, M., Montanari, G., Preti, M., Rinaldi, A., and Prevedelli, D.: The effects of sand extraction on the macrobenthos of a relict sands area (northern Adriatic Sea): results 12 months post-extraction, *Mar. Pollut. Bull.*, 50, 768–777, <https://doi.org/10.1016/j.marpolbul.2005.02.009>, 2005.
- Stouff, V., Geslin, E., Debenaj, J., and Lesourd, M.: Origin of morphological abnormalities in *Ammonia* (Foraminifera): studies in laboratory and natural environments, *J. Foramin. Res.*, 29, 152–170, <https://doi.org/10.2113/gsjfr.29.2.152>, 1999a.
- Stouff, V., Lesourd, M., and Debenay, J.-P.: Laboratory observations of asexual reproduction (schizogony) and ontogeny of *Ammonia tepida*, *J. Foramin. Res.*, 29, 75–84, <https://doi.org/10.2113/gsjfr.29.1.75>, 1999b.
- Turner, G. L. E.: The microscope as a technical frontier in science, in: *Historical Aspects of Microscopy*, edited by: Bradbury, S. and Turner, G. L. E., W. Heffer & Sons, Cambridge, 175–197, 1967.
- Tyszk, J.: Morphospace of foraminiferal shells. in: *Abstract Volume, Seventh International Workshop on Agglutinated Foraminifera*, Urbino, 2–8 October 2005, 3 pp., <https://doi.org/10.1080/00241160600575808>, 2005.
- Tyszk, J.: Morphospace of foraminiferal shells: results from the moving reference model, *Lethaia*, 39, 1–12, <https://doi.org/10.1080/00241160600575808>, 2006.
- Tyszk, J., Topa, P., and Szcza, K.: State-of-the-art in modelling of foraminiferal shells: searching for an emergent model, *Stud. Geol. Polon.*, 124, 143–157, 2005.
- von Daniels, C. H.: Quantitative Ökologische Analyse der zeitlichen und räumlichen Verteilung rezenter Foraminiferen im Limskanal bei Rovinj (nordliche Adria), *Göttinger Arbeiten zur Geologie und Paläontologie*, 8, 1–109, 1970.
- Walker, G. and Jacob, E.: in: *Essays on the Microscope*, 2nd Edition with considerable additions and improvements by F. Kammacher, edited by: Adams, E., Dillon and Keeting, London, 712 pp., 1798.
- Walton, W. R. and Sloan, B. J.: The genus *Ammonia* Brünnich 1772: Its geographic distribution and morphologic variability, *J. Foramin. Res.*, 20, 128–156, <https://doi.org/10.2113/gsjfr.20.2.128>, 1990.
- Ward, A. J. W., Webster, M. M., and Hart, P. J. B.: Intraspecific food competition in fishes, *Fish Fish.*, 7, 231–261, <https://doi.org/10.1111/j.1467-2979.2006.00224.x>, 2006.